

Theoretical and Experimental Investigations of Electromagnetic Field Distortion Due to a Perfectly Conducting Rectangular Cylinder in a Transverse Electromagnetic Cell

Motohisa Kanda

Electromagnetic Fields Division
National Engineering Laboratory
National Bureau of Standards
Boulder, Colorado 80303



U.S. DEPARTMENT OF COMMERCE, Malcolm Baldrige, Secretary

NATIONAL BUREAU OF STANDARDS, Ernest Ambler, Director

Issued April 1981

NATIONAL BUREAU OF STANDARDS TECHNICAL NOTE 1028

Nat. Bur. Stand. (U.S.), Tech. Note 1028, 48 pages (April 1981)

CODEN: NBTNAE

U.S. GOVERNMENT PRINTING OFFICE
WASHINGTON 1981

For sale by the Superintendent of Documents, U.S. Government Printing Office, Washington, D.C. 20402

Price \$2.50 (Add 25 percent for other than U.S. mailing)

TABLE OF CONTENTS

	<u>Page</u>
LIST OF FIGURES.....	iv
I. INTRODUCTION.....	2
II. THEORY	4
III. THEORETICAL AND EXPERIMENTAL RESULTS	9
IV. CONCLUSIONS	12
V. REFERENCES.....	13

LIST OF FIGURES

Figure 1.	Curve of equal TE_{01} and TE_{10} cutoff frequencies for a transverse electromagnetic cell.....	14
Figure 2.	Normalized TE_{01} cutoff wavelength for a transverse electromagnetic cell.....	15
Figure 3.	Electromagnetic field distortion due to a metallic cut in a transverse electromagnetic cell (electrostatic approximation).....	16
Figure 4.	Coordinate system of a rectangular cylinder in a parallel plate waveguide.....	17
Figure 5.	Magnetic field distortion due to a perfectly conducting cylinder (width $\lambda = 18$ cm, height $h = 5.5$ cm) in a transverse electromagnetic cell at 1 MHz.....	18
Figure 6.	Magnetic field distortion due to a perfectly conducting cylinder (width $\lambda = 18$ cm, height $h = 5.5$ cm) in a transverse electromagnetic cell at 2 MHz.....	19
Figure 7.	Magnetic field distortion due to a perfectly conducting cylinder (width $\lambda = 18$ cm, height $h = 5.5$ cm) in a transverse electromagnetic cell at 5 MHz.....	20
Figure 8.	Magnetic field distortion due to a perfectly conducting cylinder (width $\lambda = 18$ cm, height $h = 5.5$ cm) in a transverse electromagnetic cell at 10 MHz.....	21
Figure 9.	Magnetic field distortion due to a perfectly conducting cylinder (width $\lambda = 18$ cm, height $h = 5.5$ cm) in a transverse electromagnetic cell at 50 MHz.....	22
Figure 10.	Magnetic field distortion due to a perfectly conducting cylinder (width $\lambda = 18$ cm, height $h = 5.5$ cm) in a transverse electromagnetic cell at 100 MHz.....	23
Figure 11.	Magnetic field distortion due to a perfectly conducting cylinder (width $\lambda = 18$ cm, height $h = 15$ cm) in a transverse electromagnetic cell at 2 MHz.....	24
Figure 12.	Magnetic field distortion due to a perfectly conducting cylinder (width $\lambda = 18$ cm, height $h = 15$ cm) in a transverse electromagnetic cell at 5 MHz.....	25
Figure 13.	Magnetic field distortion due to a perfectly conducting cylinder (width $\lambda = 18$ cm, height $h = 15$ cm) in a transverse electromagnetic cell at 10 MHz.....	26

Figure 14.	Magnetic field distortion due to a perfectly conducting cylinder (width $\lambda = 18$ cm, height $h = 15$ cm) in a transverse electromagnetic cell at 50 MHz.....	27
Figure 15.	Magnetic field distortion due to a perfectly conducting cylinder (width $\lambda = 18$ cm, height $h = 15$ cm) in a transverse electromagnetic cell at 100 MHz.....	28
Figure 16.	Magnetic field distortion due to a perfectly conducting cylinder (width $\lambda = 18$ cm, height $h = 25$ cm) in a transverse electromagnetic cell at 2 MHz.....	29
Figure 17.	Magnetic field distortion due to a perfectly conducting cylinder (width $\lambda = 18$ cm, height $h = 25$ cm) in a transverse electromagnetic cell at 5 MHz.....	30
Figure 18.	Magnetic field distortion due to a perfectly conducting cylinder (width $\lambda = 18$ cm, height $h = 25$ cm) in a transverse electromagnetic cell at 10 MHz.....	31
Figure 19.	Magnetic field distortion due to a perfectly conducting cylinder (width $\lambda = 18$ cm, height $h = 25$ cm) in a transverse electromagnetic cell at 50 MHz.....	32
Figure 20.	Magnetic field distortion due to a perfectly conducting cylinder (width $\lambda = 18$ cm, height $h = 25$ cm) in a transverse electromagnetic cell at 100 MHz.....	33
Figure 21.	Magnetic field distortion at the center of the top of the cylinder as the ratio of its height to the separation distance of the parallel plate waveguide at 2 MHz.....	34
Figure 22.	Magnetic field distortion at the center of the top of the cylinder as the ratio of its height to the separation distance of the parallel plate waveguide at 5 MHz.....	35
Figure 23.	Magnetic field distortion at the center of the top of the cylinder as the ratio of its height to the separation distance of the parallel plate waveguide at 10 MHz.....	36
Figure 24.	Magnetic field distortion at the center of the top of the cylinder as the ratio of its height to the separation distance of the parallel plate waveguide at 50 MHz.....	37
Figure 25.	Magnetic field distortion at the center of the top of the cylinder as the ratio of its height to the separation distance of the parallel plate waveguide at 100 MHz....	38
Figure 26.	Electric field distortion at the center of the top of the cylinder as the ratio of its height to the separation distance of the parallel plate waveguide.....	39

Figure 27.	Simultaneous electric and magnetic field measurements using a doubly-loaded electrically small loop.....	40
Figure 28.	Phase degradation of the TEM mode as the ratio of the cylinder height to the separation distance between the center conductor and the ground plane in the TEM cell.....	41

Theoretical and Experimental Investigations of Electromagnetic Field
Distortion Due to a Perfectly Conducting Rectangular
Cylinder in a Transverse Electromagnetic Cell

Motohisa Kanda

Electromagnetic Fields Division
National Bureau of Standards
Boulder, Colorado 80303

The study of electromagnetic compatibility (EMC), that is the electronic and biological effects due to electromagnetic (EM) radiation, and EM calibration require accurate EM measurement techniques for defining the EM interference (EM) characteristics. Thus, fully enclosed rectangular transverse electromagnetic (TEM) transmission lines with thin inner conductors are often used for generating standard known test fields. In all cases it is desirable that only the dominant TEM mode should propagate.

In the EMC measurements, an object under test is placed inside of a TEM cell. The field from the TEM mode incident upon this scattering object is identical to that of a plane wave in a free space. However, the scattered field produced by the object in the TEM cell is different from the scattered field produced by the object in a free space, because of multiple reflections from the TEM cell walls, or equivalently, the mutual coupling between the object and the TEM cell.

The purpose of this paper is to discuss the loading effects, i.e., the electromagnetic field distortion caused by an object under test in a TEM cell. In the theoretical analysis, the frequency domain integral equation for the magnetic field, or equivalently, the current density on the surface of a perfectly conducting cylinder in a parallel plate waveguide is solved by the method of moments to predict the degree of magnetic field distortion.

The experimental investigations are performed by mounting a number of electrically small half loops on the surface of the perfectly conducting cylinder in a TEM cell. The loading effects in terms of magnetic field distortion are analyzed as the ratio of one of the object dimensions (height) to the separation distance between the inner conductor and the ground plane of the TEM cell. Also, the response of an electrically small loop to both the magnetic and electric components of the electromagnetic

field is used to measure the phase relation between the magnetic and electric fields, which in turn can be used to determine the degree of degradation of the TEM mode due to the presence of the perfectly conducting cylinder. These theoretical and experimental results are compared with the available quasi electrostatic results.

Keywords: Electromagnetic Compatibility (EMC); Green's function; integral equation; linear equation; method of moments; parallel plate waveguide; quasi electrostatic; TEM cell.

I. INTRODUCTION

The study of electromagnetic compatibility (EMC), that is the electric and biological effects due to electromagnetic (EM) radiation, and EM calibration require accurate EM measurement techniques for defining the EM interference (EMI) characteristics. Thus, fully enclosed rectangular transverse electromagnetic (TEM) transmission lines with thin inner conductors are often used for generating standard known test fields. In all cases, it is desirable that only the dominant TEM mode should propagate. Thus, the usefulness of these structures is limited to a frequency region below some upper frequency bound in order to suppress the higher order modes.

The higher order mode cutoff frequencies of the rectangular TEM cell have been well studied by many workers [1,2,3,4]. While in a rectangular hollow waveguide, the dominant mode is always the TE_{10} mode as long as the width exceeds the height, the same conclusion does not hold for the rectangular line with an inner conductor even if its thickness is infinitesimally small. In fact, it is found [1,2,4] that, depending on the width of the inner conductor and the size of the TEM cell, the cutoff frequency of the TE_{01} mode can be much lower than that

of the TE_{10} mode as illustrated in figure 1. While the cutoff frequency of the TE_{10} mode is simply calculated from

$$f_c = \frac{1}{2\sqrt{\mu\epsilon}} \sqrt{\left(\frac{m}{a}\right)^2 + \left(\frac{n}{b}\right)^2} \bigg|_{\substack{m=1 \\ n=0}} = \frac{1}{2a\sqrt{\mu\epsilon}}, \quad (1)$$

the cutoff frequencies of the TE_{01} mode are much more involved and have been calculated by many workers [1,2,3,4] as shown in figure 2. Let us consider, for example, a typical 50 Ω TEM cell having a width of $a = 1$ m, a height of $b = 0.6$ m, and a width of inner conductor of $s = 0.72$ m. While the cutoff frequency of the TE_{10} mode is 150 MHz, the cutoff frequency of the TE_{01} mode is approximately 135 MHz according to figure 2. It can also be shown that the cutoff frequencies of all TM modes of a TEM cell are always higher than those of their hollow waveguide counterparts. Thus, the dominant cutoff frequency (i.e., the lowest) is either the TE_{01} mode or the TE_{10} mode. It is interesting to note that the cutoff frequency of the TE_{01} mode decreases as the gap between the inner conductor and the wall of the TEM cell becomes narrower. This phenomenon has also been observed in a ridge waveguide [5] and is associated with the infinite gap capacitance.

In the EMC measurements, an object under test is placed inside of a TEM cell. The field from the TEM mode incident upon the scattering object is identical to that of a plane wave in a free space. However, the scattered field produced by the object in the TEM cell is different from the scattered field produced by the object in a free space because of multiple reflections from the TEM cell walls, or equivalently, the mutual coupling between the object and the TEM cell.

Placing a test object in a TEM cell is equivalent to introducing a capacitive discontinuity. For low frequencies, where the transverse dimensions of the object are negligible compared to the wavelength, the discontinuity due to the object is a pure capacitive reactance, and may be regarded as the fringing capacitance of the corresponding electrostatic problems. Under this assumption, the ratio of the electric field strength near the metal object in the TEM cell to the unperturbed electric field strength at the same location in a pure TEM mode has been calculated by G. Meyer [6] and is shown in figure 3.

The purpose of this paper is to discuss the loading effects, i.e., the electromagnetic field distortion caused by an object under test in a TEM cell. In the theoretical analysis, the frequency domain integral equation for the magnetic field, or equivalently, the current density on the surface of a perfectly conducting cylinder in a parallel plate waveguide is solved by the method of moments to predict the degree of magnetic field distortion. For the purpose of mathematical tractability, a parallel plate waveguide is used to model a TEM cell structure. The results given in the paper are for the magnetic field intensity on the surface of the cylinder. Other related quantities, such as the electric field intensity and the poynting vector, can be readily derived from the surface current by use of Maxwell's equations.

II. THEORY

The problem of determining the electromagnetic field scattered by a perfectly conducting rectangular cylinder has been studied by many

workers [7,8,9]. The coordinate system used to analyze the current density on the surface of the rectangular cylinder in a parallel plate waveguide is shown in figure 4. The source of the TEM wave is a delta function voltage source of the form

$$\vec{M} = \vec{y} V_0(\omega) \delta(z - z_0), \quad (2)$$

where V_0 is the magnitude of an equivalent voltage source located at the source location z_0 . Since there is no variation in the y direction and the voltage source has only a y -component, we will have a scalar wave equation in H_y , i.e.,

$$\nabla^2 H_y + k^2 H_y = j\omega\epsilon M_y, \quad (3)$$

where $\nabla^2 = \frac{\partial^2}{\partial x^2} + \frac{\partial^2}{\partial z^2}$ and k is the free space wave number. The boundary condition is that the normal \vec{H} field be zero on all of the reflecting conducting surfaces, i.e.

$$\frac{\partial H_y}{\partial n} = 0, \quad (4)$$

where $n = x$ and z .

The solution of equation (3) may be found through the Green's Function technique,

$$\nabla^2 G(r, r') + k^2 G(r, r') = -\delta(x-x') \delta(z-z'). \quad (5)$$

Multiplying eq. (3) by $G(r, r')$, eq. (5) by H_y , subtracting the two results and integrating over the free space volume V ,

$$\begin{aligned} & \int_V [G(r, r') \nabla^2 H_y(r') - H_y(r') \nabla^2 G(r, r')] dv' \\ & = j\omega\epsilon \int_V G(r, r') M_y(r') dv' + \int_V H_y(r') \delta(x-x') \delta(z-z') dv'. \end{aligned} \quad (6)$$

Evaluating the integration of the right hand side of eq. (6) and using Green's theorem on the left hand side, we get

$$\begin{aligned} & \int_S [G(r, r') \frac{\partial H_y(r')}{\partial n'} - H_y(r') \frac{\partial G(r, r')}{\partial n'}] ds' \\ & = j\omega\epsilon \int_V G(r, r') M_y(r') dv' + H_y(r). \end{aligned} \quad (7)$$

On the perfectly conducting surface, s , of the plates, we set the boundary condition as

$$\frac{\partial H_y(r')}{\partial n'} = 0. \quad (8)$$

Equation 7 then reduces to

$$H_y(r) = -j\omega\epsilon \int_V G(r, r') M_y(r') dv' - \int_{s_c} H_y(r') \frac{\partial G(r, r')}{\partial n'} ds', \quad (9)$$

where s_c indicates the surface of the rectangular cylinder. The first term on the right hand side of eq. (9) corresponds to the incident field, and the second term to the scattered field. The known incident

magnetic field is given by

$$\begin{aligned}
 H^{inc}(x,z) &= -j\omega\epsilon \int_0^\infty \int_0^b V_0 \delta(z'-z_0) G(x,z; x',z') dx' dz' \\
 &= \frac{\omega\epsilon}{k} V_0 e^{jkz_0} \cos kz.
 \end{aligned} \tag{10}$$

Equation (9) is an integral equation which can be solved for $H_y(r)$ once Green's function $G(r,r')$ is obtained.

The Green's function is the solution of eq. (5). By imposing the proper boundary condition for the parallel plate waveguide, i.e.

$$\frac{\partial G}{\partial x} = 0 \tag{11}$$

at $x=0$ and $x=b$, then one finds [10]

$$\begin{aligned}
 G(x,z;x',z') &= \frac{j}{2kb} [e^{jk(z+z')} + e^{jk|z-z'|}] \\
 &+ \frac{j}{b} \sum_{n=1}^{\infty} \frac{\cos \frac{n\pi x}{b} \cos \frac{n\pi x'}{b}}{\Gamma_n} [e^{j\Gamma_n(z+z')} + e^{j\Gamma_n|z-z'|}],
 \end{aligned} \tag{12}$$

where

$$\Gamma_n = \sqrt{k^2 - \left(\frac{n\pi}{b}\right)^2}. \tag{13}$$

Once the Green's function is obtained and the source is specified, eq. (9) can be solved by the method of moments. The technique used is discussed briefly below. A detailed discussion on this subject is given

by Harrington [11].

The unknown H_y is expanded in terms of a set of known basis functions f_i with unknown coefficients α_i , i.e.

$$H_y = \sum_{i=1}^n \alpha_i f_i. \quad (14)$$

Substituting eq. (14) into eq. (9) we obtain

$$\sum_{i=1}^n \alpha_i [f_i(x, z) + \int_{S'} f_i(x', z') \frac{\partial G(x, z; x', z')}{\partial n'} ds'] = H^{inc}(x, z). \quad (15)$$

Equation (15) is a single equation with n unknown α_i . To create at least n linear equations, a set of testing function, w_j , is introduced, and the inner products (integral over the surface) of both sides of eq. (15) for each w_j are set equal. This forms a set of linear equations of the form

$$[Z] [I] = [V], \quad (16)$$

where the matrix element Z_{ij} is given by

$$Z_{ij} = \int_S [f_i(r) + \int_{S'} f_i(r') \frac{G(r, r')}{\partial n'} ds'] w_j(r) ds, \quad (17)$$

and the column matrix element V_j is given by

$$V_j = \int_S H^{inc}(r) w_j(r) ds. \quad (18)$$

The unknown coefficients α_j are found by solving the matrix eq (16).

The expression for H_y is then given by eq (14).

III. THEORETICAL AND EXPERIMENTAL RESULTS

A number of electrically small half loops whose diameters are 1.5 cm are mounted transversely across a perfectly conducting rectangular cylinder. The cylinder is placed in a TEM cell which acts approximately as a parallel plate waveguide. A vector voltmeter is used to measure both the magnitude and phase of the magnetic field strength and therefore the current density on the surface of the cylinder. In the theoretical analysis, the frequency domain integral equation for the magnetic field on the surface of the cylinder in a parallel plate waveguide given in section II is solved by the method of moments. Other related quantities, such as the electric field intensity and the poynting vector can be readily derived from the surface current by use of Maxwell's equations.

In this paper, the loading effects due to the perfectly conducting rectangular cylinder in a TEM cell are indicated in terms of the magnetic field distortion, which is defined as the ratio of the magnetic field strength on the surface of the cylinder in a TEM cell to that at the same position in an empty TEM cell. In this paper, the separation distance of the parallel plate waveguide, i.e., the distance between the center conductor and the ground plane in the TEM cell is chosen to be 30 cm. Three different perfectly conducting rectangular cylinders are used, all of which have the same widths of 18 cm, but have different heights of 5.5 cm, 15 cm, and 18 cm. The magnetic field distortion and

the corresponding phase are shown in figures 5 through 20 for frequencies from 1 MHz to 100 MHz. The phase reference is taken to be at the center of the top of the cylinder ($x=h$ and $\frac{\lambda}{2}$). Figures 21 through 25 show the magnetic field distortion at the center of the top of the cylinder as the ratio of its height to the separation distance of the TEM cell. For a comparison, the electric field distortion due to a metal cube reported by G. Meyer [6] is also shown in these figures. In general, it is found that the magnetic field distortion due to a perfectly conducting rectangular cylinder is quite small and much less than the electric field distortion reported by G. Meyers [6].

In order to confirm the result by G. Meyer [6], a electrically small dipole is mounted on the center of the top of the perfectly conducting rectangular cylinder. The electric field distortion (defined as the ratio of electric field at the surface of the cylinder to that at the same position in an empty TEM cell) is shown in figure 26 as the ratio of the cylindrical height to the separation distance of the parallel plate waveguide. Figure 26 indicates that the electric field distortion is much larger than that predicted by G. Meyer [6]. The discrepancy may be due to the fact that the Meyer calculation is based on the quasi electrostatic approximation.

When the perfectly conducting rectangular cylinder is placed in the TEM cell, the scattered field produced by the cylinder can be far different from the original incident TEM mode. In order to determine the degree of degradation of the TEM mode due to the presence of the cylinder, the response of an electrically small loop to both the magnetic and electric components of an electromagnetic field is

examined. Consider the loop loaded at each of the diametrically opposite points as shown in figure 27. One can show that the sum of the two load currents I_{Σ} is given by [12]

$$I_{\Sigma} = K_h H_y, \quad (19)$$

and their difference I_{Δ} is given as

$$I_{\Delta} = K_e E_x, \quad (20)$$

where K_h and K_e are, respectively, the loop sensitivity constant for magnetic and electric fields. These formulas clearly show that the use of the sum current gives a measure of the magnetic field, whereas that of its difference gives a measure of the electric field.

While the phase between magnetic and electric field is normally in phase for the pure TEM mode, the presence of the perfectly conducting rectangular cylinder in the TEM cell will cause a distortion and thus a phase degradation of the TEM mode around the cylinder. The phase degradation of the TEM mode thus obtained is shown in figure 28 as the ratio of the cylinder height to the separation distance of the TEM cell. It is very interesting to note that the phase degradation at the center of the cylinder becomes predominant as the frequency approaches to the cutoff frequency of the TE_{01} mode and also the height of the cylinder becomes comparably large compared to the separation of the parallel plate waveguide. The phase degradation observed at the low frequencies around 2 MHz is not well understood, but is probably due to the experi-

mental problems caused by the vector voltmeter and the hybrid junction used in the experiments.

IV. CONCLUSIONS

This paper discussed the loading effects, i.e., the electromagnetic field distortion caused by a metal object placed in a TEM cell. In the theoretical analysis, the frequency domain integral equation for the magnetic field intensity on the surface of a perfectly conducting cylinder in a parallel plate waveguide was solved by the method of moments to obtain the degree of magnetic field distortion. The results given in the paper are for the magnetic field intensity on the surface of the cylinder. Other related quantities, such as the electric field intensity and the poynting vector can be readily derived from the surface current by use of Maxwell's equations.

The experimental investigations were performed by mounting a number of electrically small half loops on the surface of a perfectly conducting cylinder placed in a TEM cell. The loading effects in terms of magnetic field distortion were expressed as the ratio of the object height to the separation distance between the inner conductor and the ground plane of the TEM cell. Also, the response of an electrically small loop to both the magnetic and electric components of an electromagnetic field was used to measure the phase relation between the magnetic and electric fields, which in turn was used to assess the degree of degradation of the TEM mode due to the presence of the perfectly conducting cylinder. These theoretical and experimental

results were compared with the available quasi electrostatic results.

V. REFERENCES

- [1] Brackelmann, W., Landmann, D., and Schlosser, W., Die Grenzfrequenzen von höheren Eigenwellen in Streifenleitungen AEU, Vol. 21, pp 112-120 (March 1967).
- [2] Gruner, L., High Order Modes in Rectangular Coaxial Waveguides, IEEE Trans. Microwave Theory Technique, Vol MTT-15, pp. 483-485, (August 1967).
- [3] Mittra, R., and Itoh, T., A New Technique for the Analysis of the Dispersion Characteristics of Microstrip Lines, IEEE Trans. Microwave Theory Technique, Vol MTT-19, pp. 47-56, (January 1971).
- [4] Tippet, J. C., Modal Characteristics of Rectangular Coaxial Transmission Line, Ph.D Thesis, University of Colorado, Boulder, CO. (June 1978).
- [5] Ramo, S., and Whinnery, J. R., Fields and Waves in Modern Radio, 2nd Edition, John Wiley & Sons, Inc., New York, N. Y. (1953).
- [6] Meyer, G., Application of a Broadband Measuring Line in Field Immunity Testing, 2nd Symposium and Technical Exhibition on Electromagnetic Compatibility, Montreux, Switzerland, pp. 241-46, (June 1977).
- [7] Mei, K., and Van Bladel, J. G., Low-Frequency Scattering by Rectangular Cylinders, IEEE Trans. Antennas and Propagation, Vol. AP-11, pp. 52-56, (January 1963).
- [8] Mei, K. K. and Van Bladel, J. G., Scattering by Perfectly Conducting Rectangular Cylinders, IEEE Trans. Antennas and Propagation, Vol. AP-11, pp. 185-192, (March 1963).
- [9] Andreasen, M. G., Comments on Scattering by Conducting Rectangular Cylinders, IEEE Trans. Antennas and Propagation, Vol. AP-12, pp. 235-236, (March 1964).
- [10] Morse, P. M. and Feshbach, H., Methods of Theoretical Physics, McGraw-Hill Book Company, Inc., New York, (1953).
- [11] Harrington, R. F., Field Computation by Moment Methods, the Macmillan Company, New York, (1968).
- [12] Whiteside, H. and King, R.W.P., The Loop Antenna as a Probe, IEEE Trans. Antennas and Propagation, Vol. AP-19, No. 3, pp. 291-297, (May 1964).

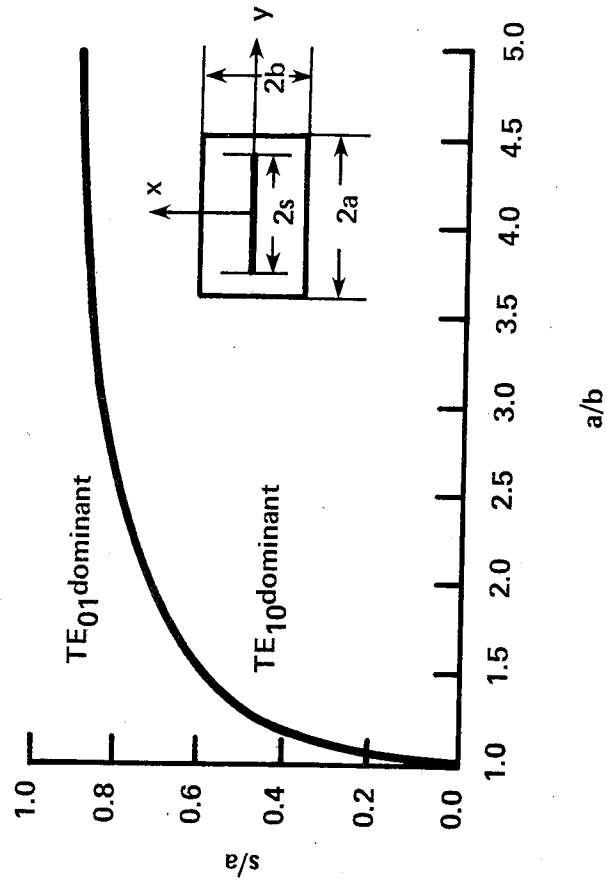


Figure 1. Curve of equal TE_{01} and TE_{10} cutoff frequencies for a transverse electromagnetic cell.

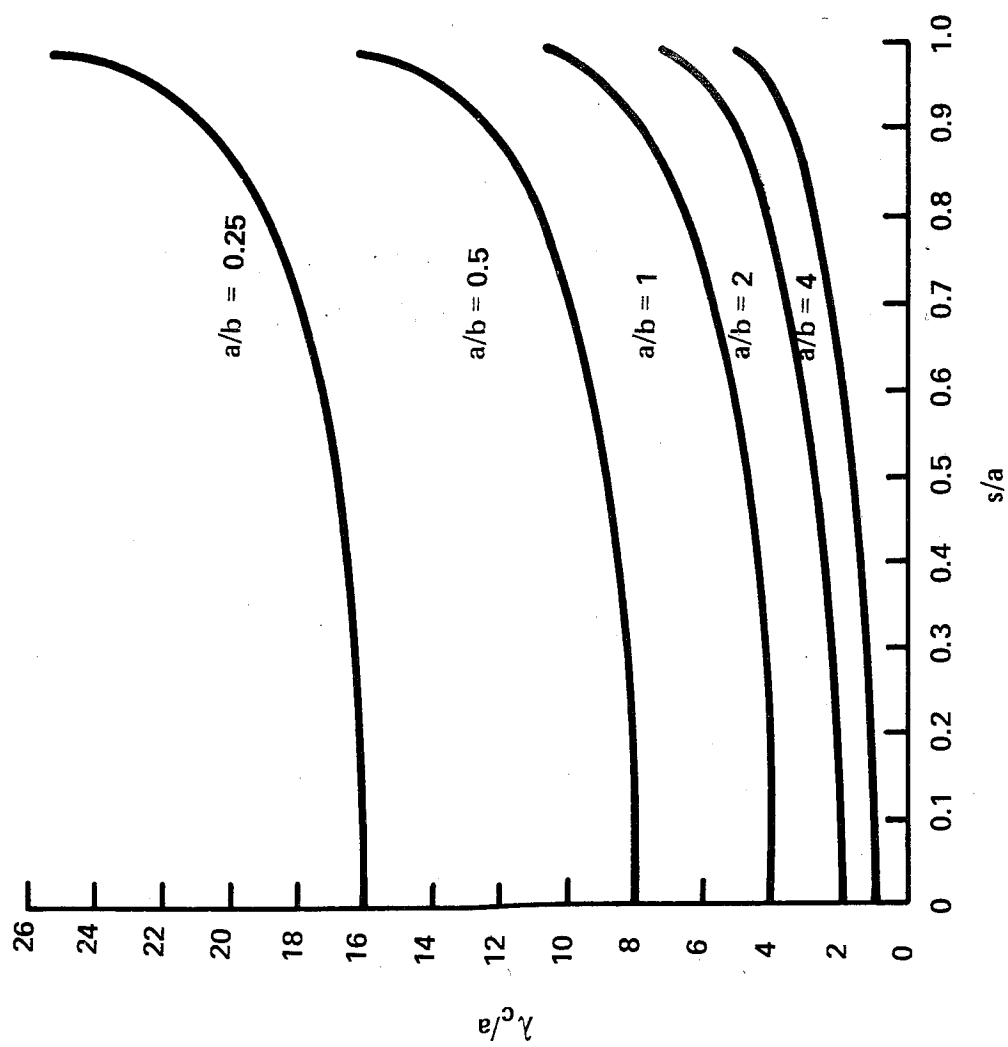


Figure 2. Normalized TE₀₁ cutoff wavelength for a transverse electromagnetic cell.

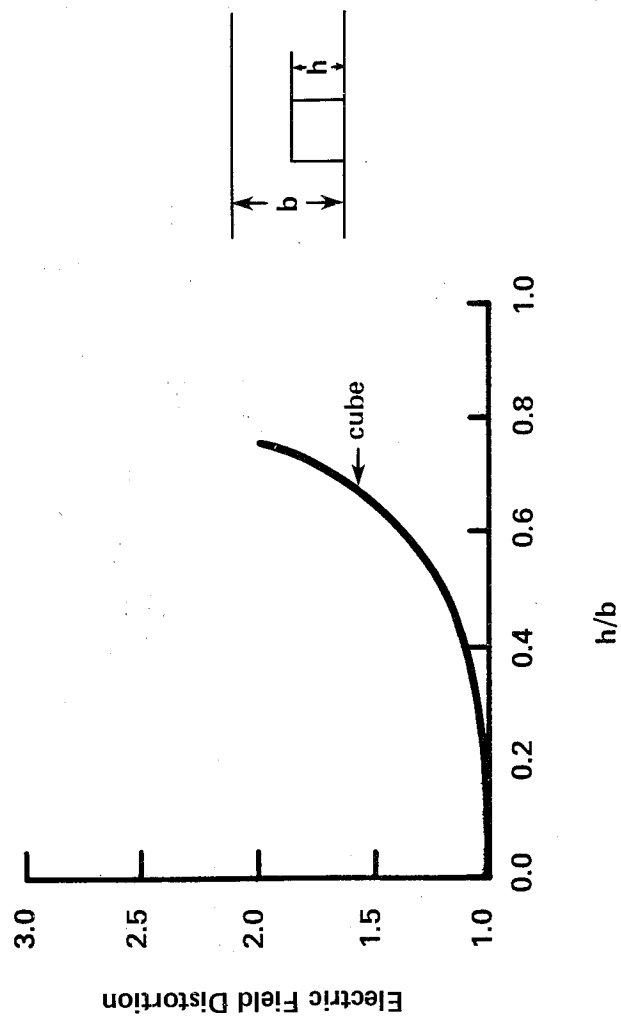


Figure 3. Electromagnetic field distortion due to a metallic cut in a transverse electromagnetic cell (electrostatic approximation).

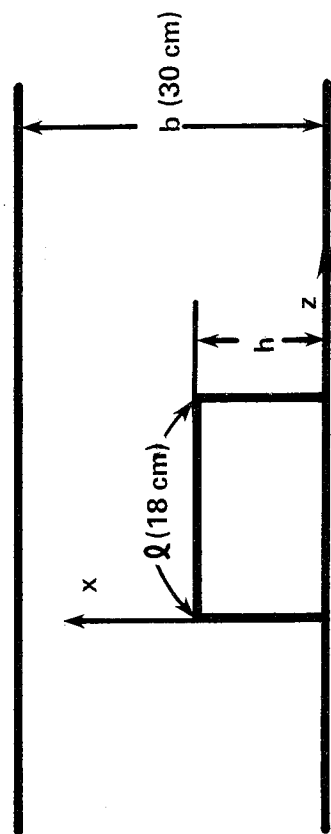


Figure 4. Coordinate system of a rectangular cylinder in a parallel plate waveguide.

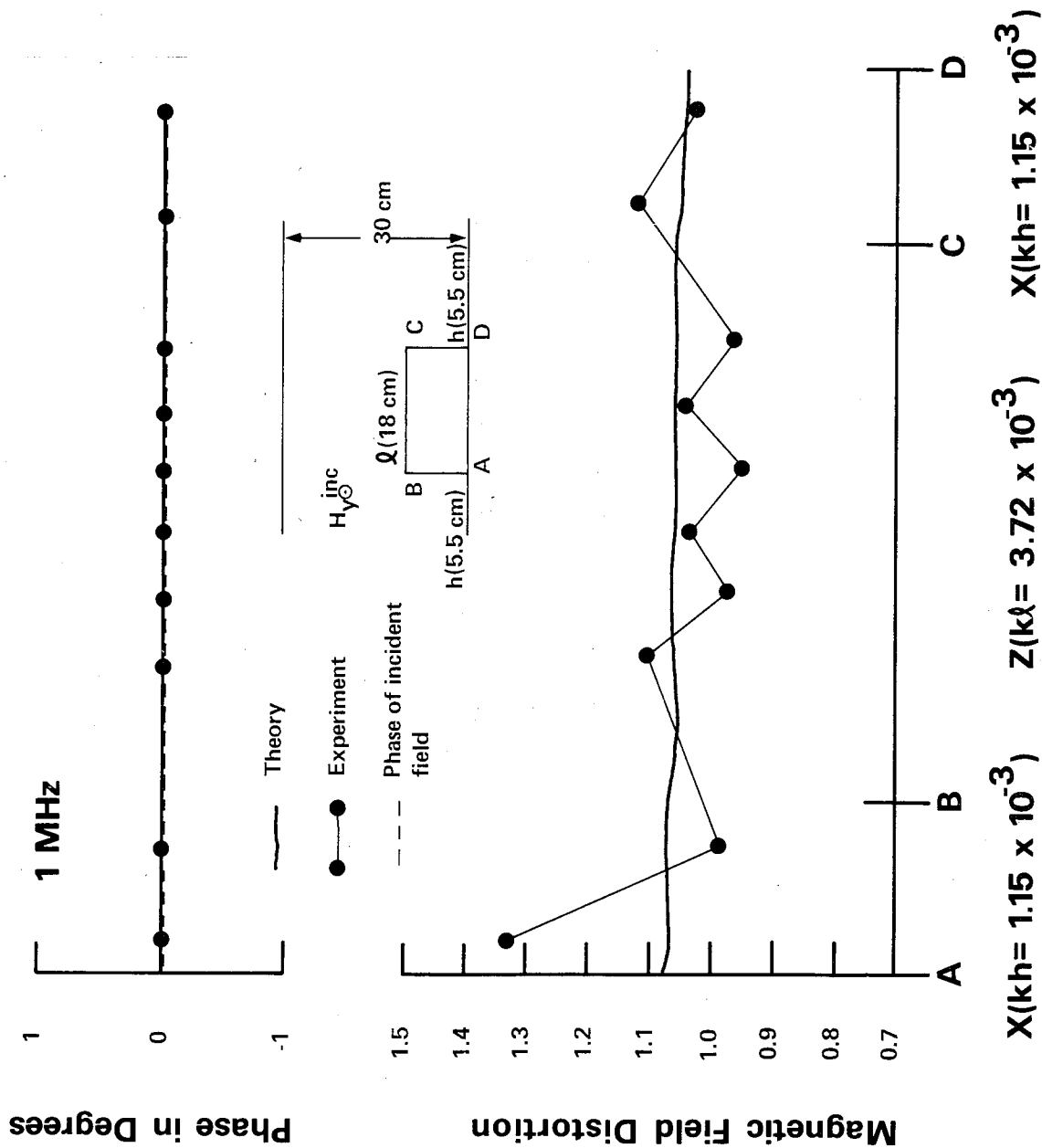


Figure 5. Magnetic field distortion due to a perfectly conducting cylinder (width $\ell = 18 \text{ cm}$, height $h = 5.5 \text{ cm}$) in a transverse electromagnetic cell at 1 MHz .

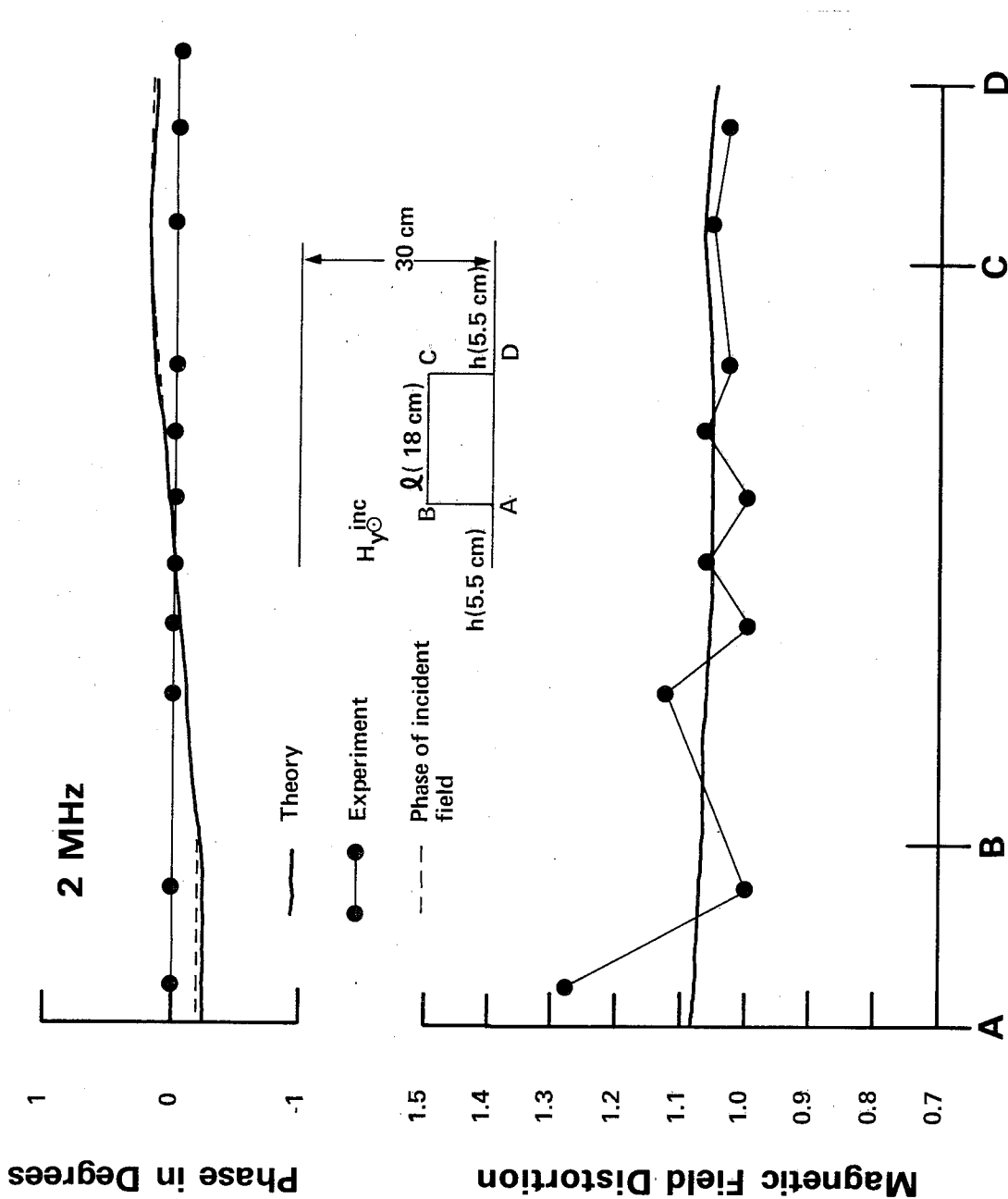


Figure 6. Magnetic field distortion due to a perfectly conducting cylinder (width $l = 18$ cm, height $h = 5.5$ cm) in a transverse electromagnetic cell at 2 MHz.

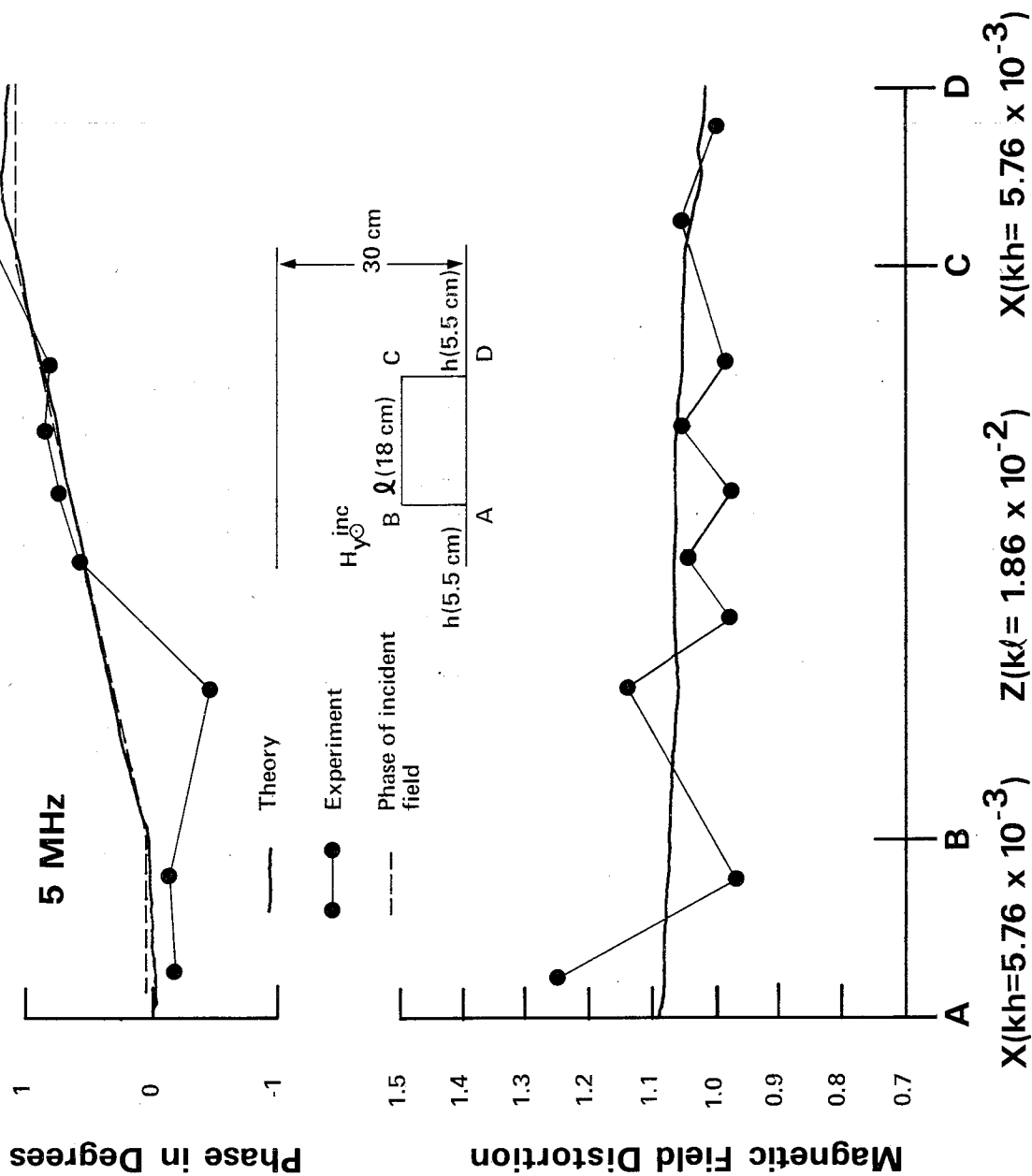


Figure 7. Magnetic field distortion due to a perfectly conducting cylinder (width $l = 18$ cm, height $h = 5.5$ cm) in a transverse electromagnetic cell at 5 MHz.

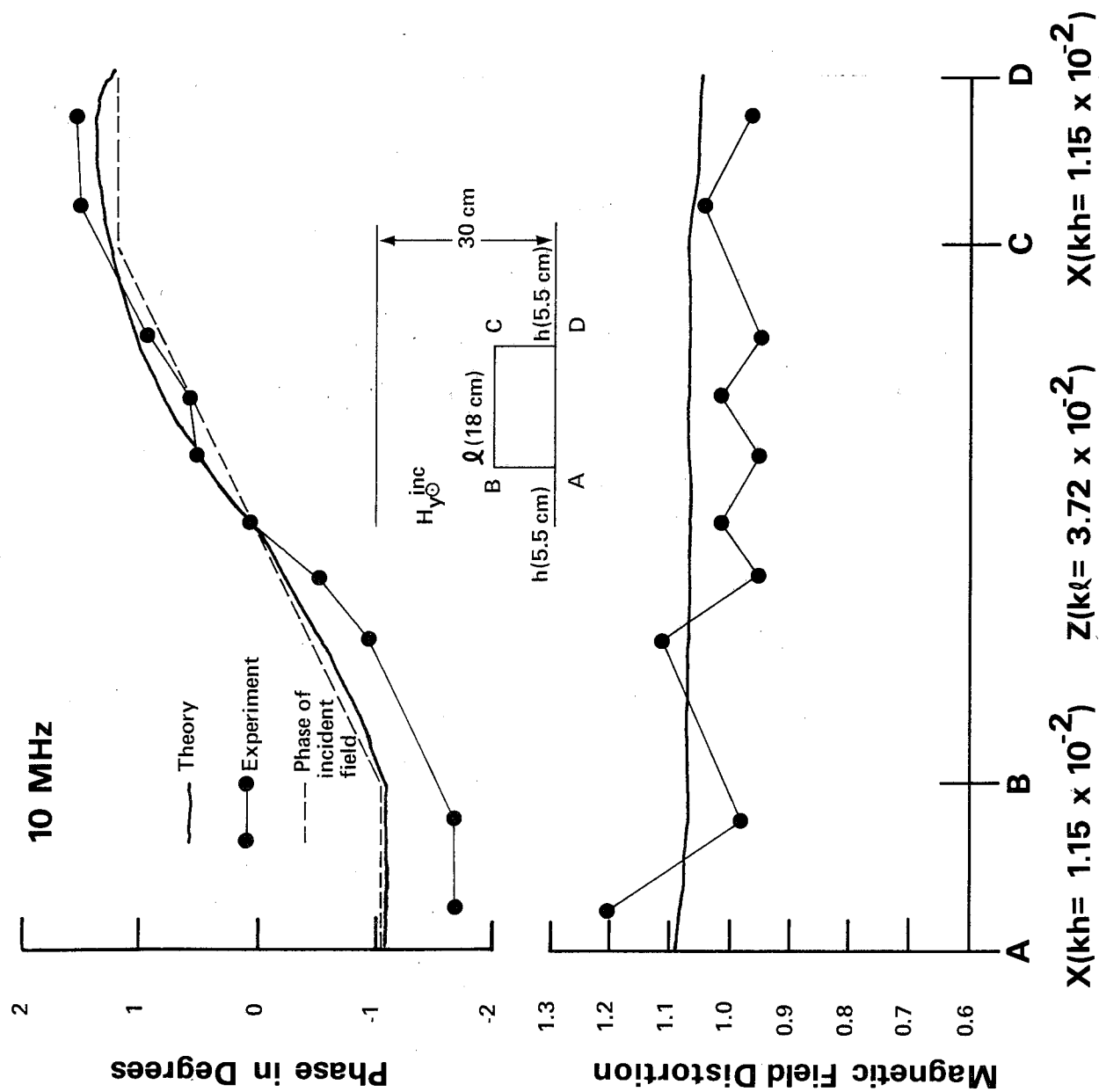


Figure 8. Magnetic field distortion due to a perfectly conducting cylinder (width $\ell = 18$ cm, height $h = 5.5$ cm) in a transverse electromagnetic cell at 10 MHz.

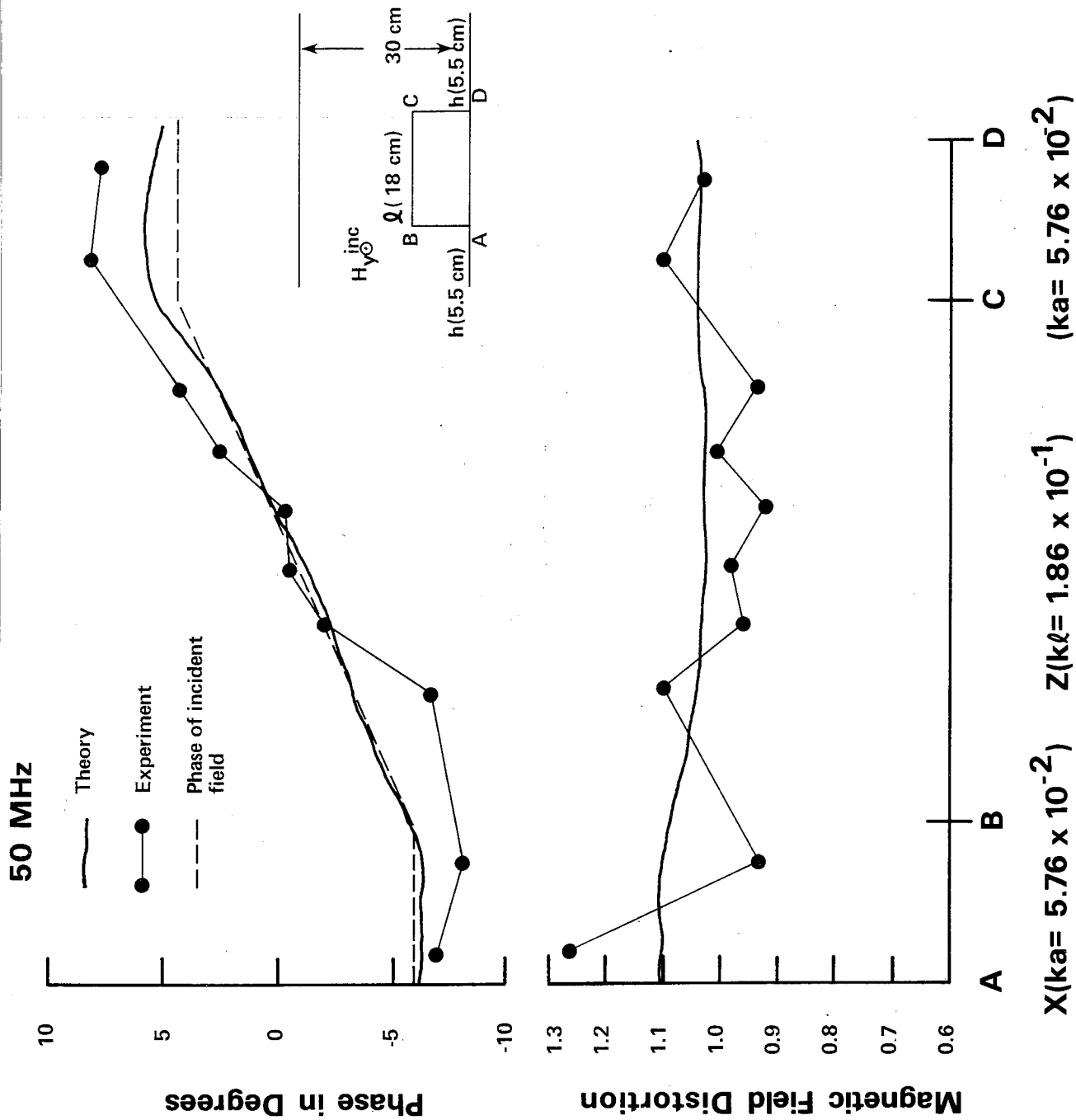


Figure 9. Magnetic field distortion due to a perfectly conducting cylinder (width $\ell = 18 \text{ cm}$, height $h = 5.5 \text{ cm}$) in a transverse electromagnetic cell at 50 MHz.

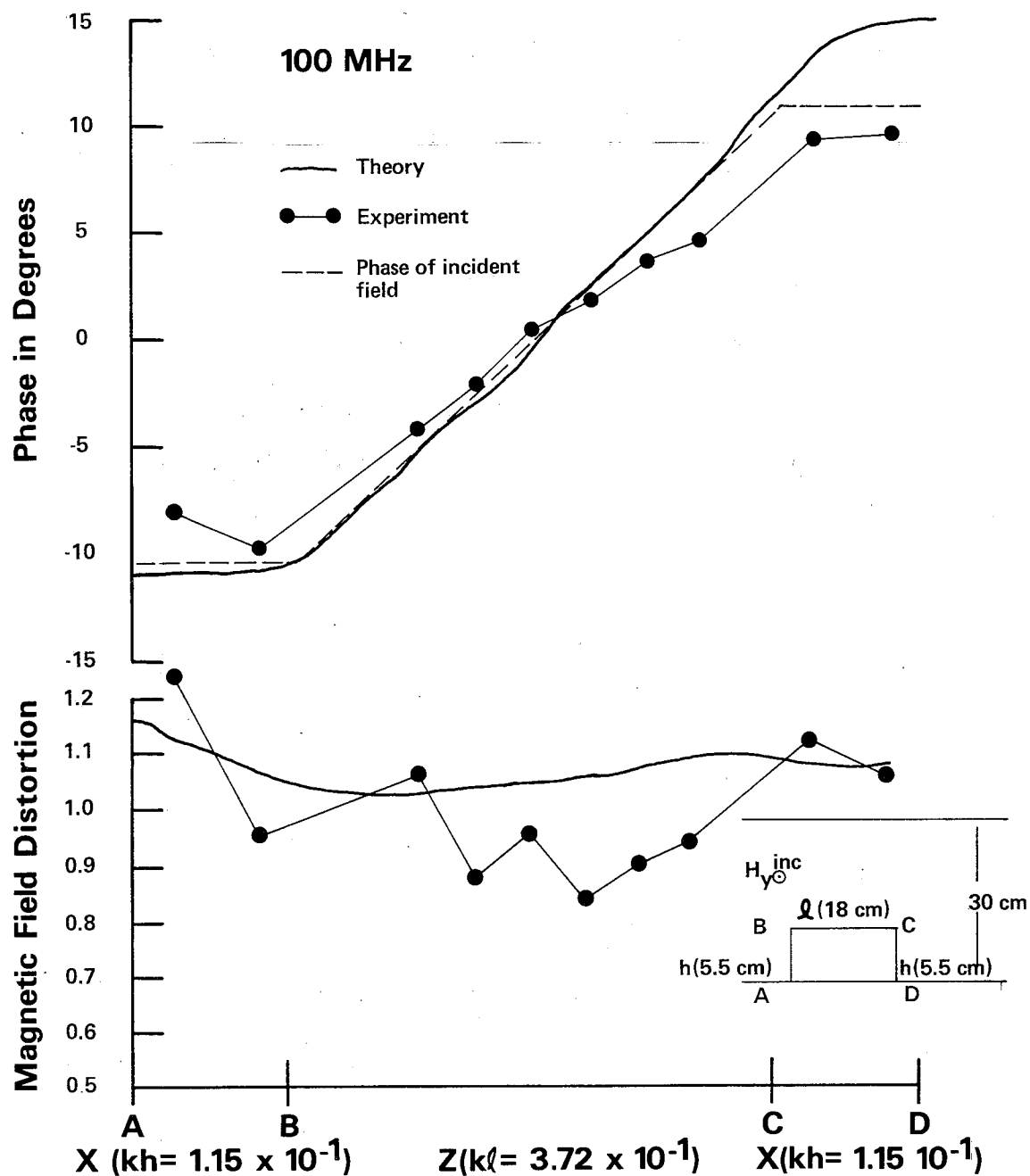


Figure 10. Magnetic field distortion due to a perfectly conducting cylinder (width $l = 18 \text{ cm}$, height $h = 5.5 \text{ cm}$) in a transverse electromagnetic cell at 100 MHz.

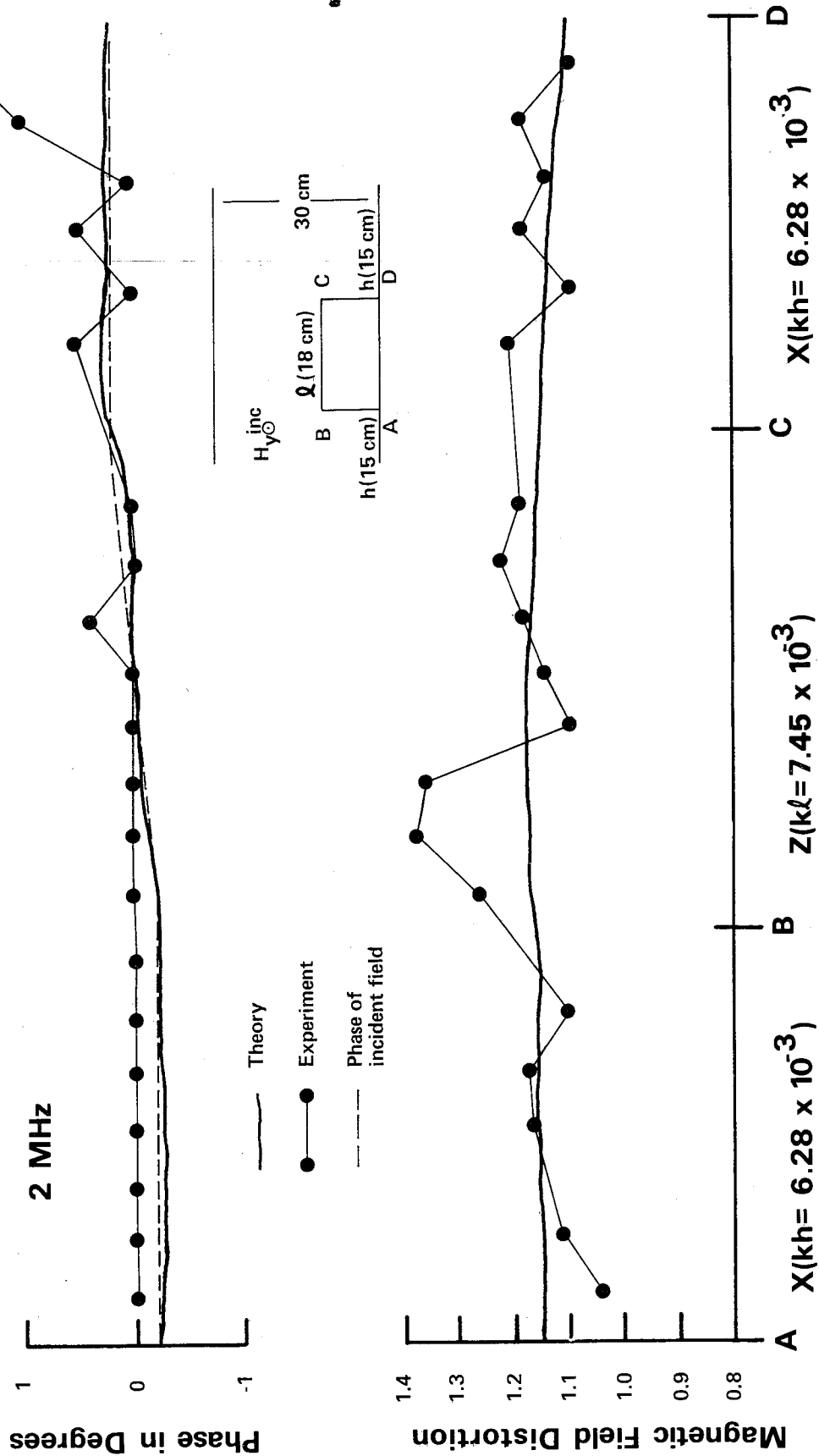


Figure 11. Magnetic field distortion due to a perfectly conducting cylinder (width $\lambda = 18$ cm, height $h = 15$ cm) in a transverse electromagnetic cell at 2 MHz.

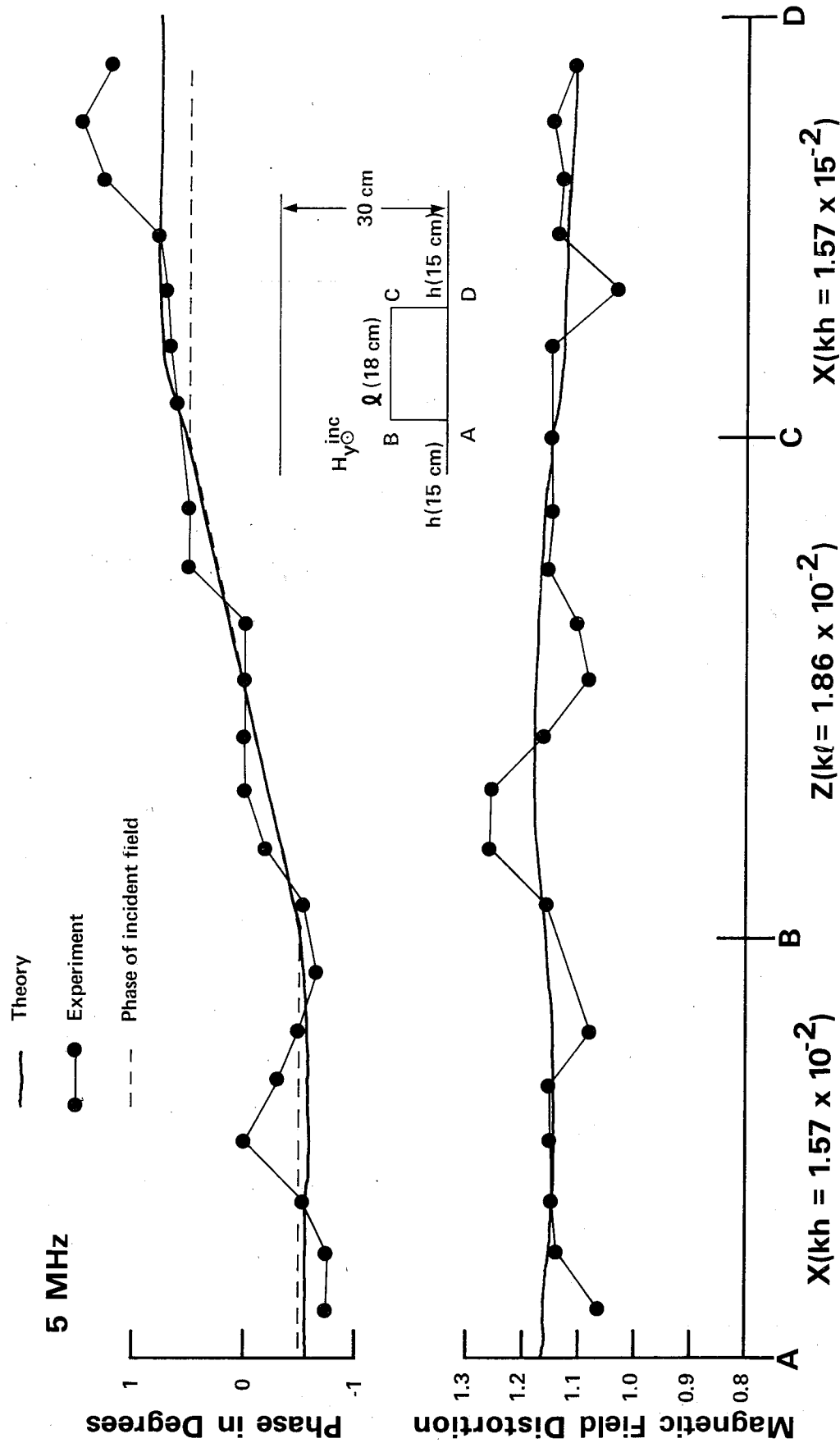


Figure 12. Magnetic field distortion due to a perfectly conducting cylinder (width $\lambda = 18$ cm, height $h = 15$ cm) in a transverse electromagnetic cell at 5 MHz.

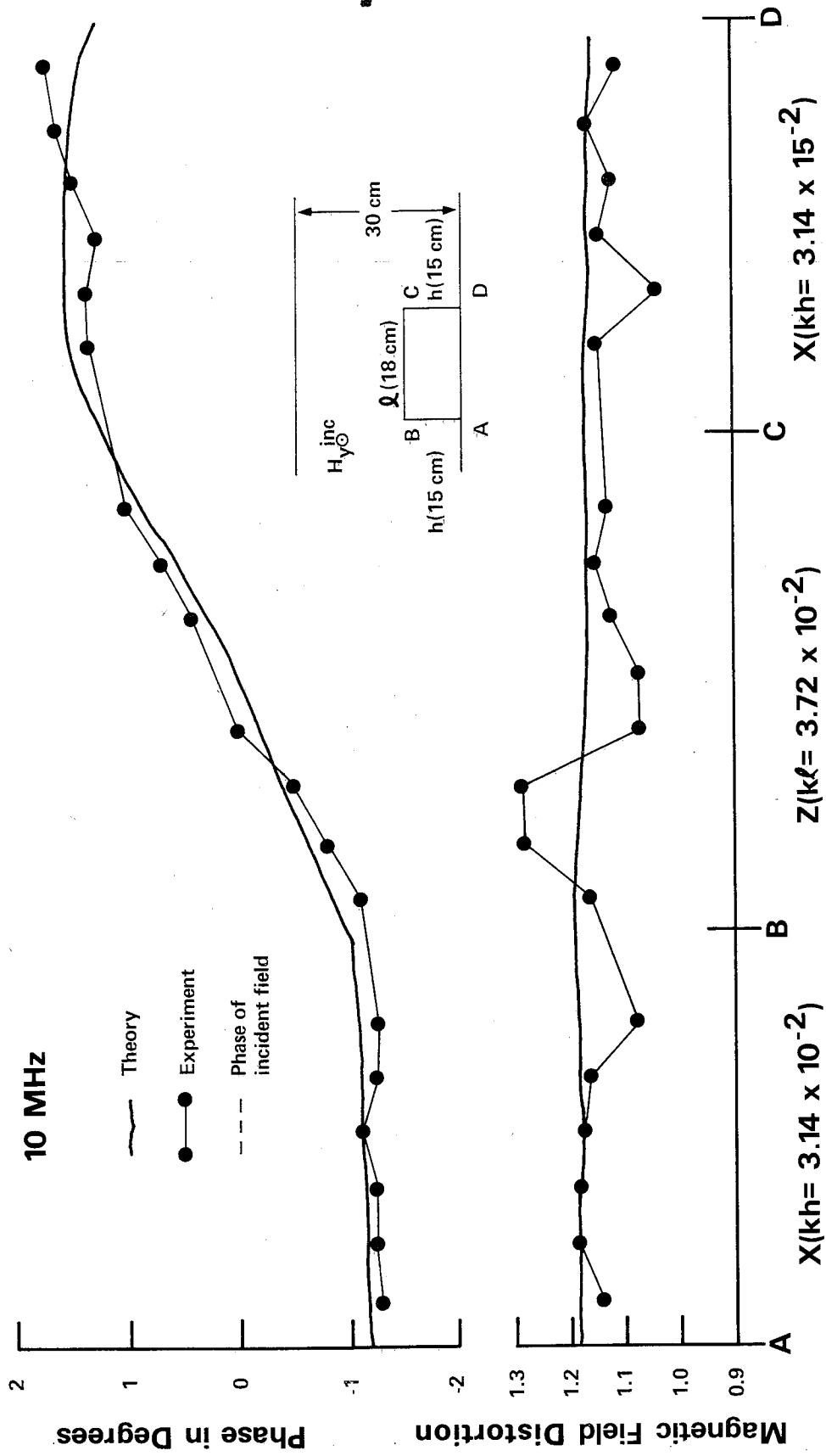


Figure 13. Magnetic field distortion due to a perfectly conducting cylinder (width $l = 18$ cm, height $h = 15$ cm) in a transverse electromagnetic cell at 10 MHz.

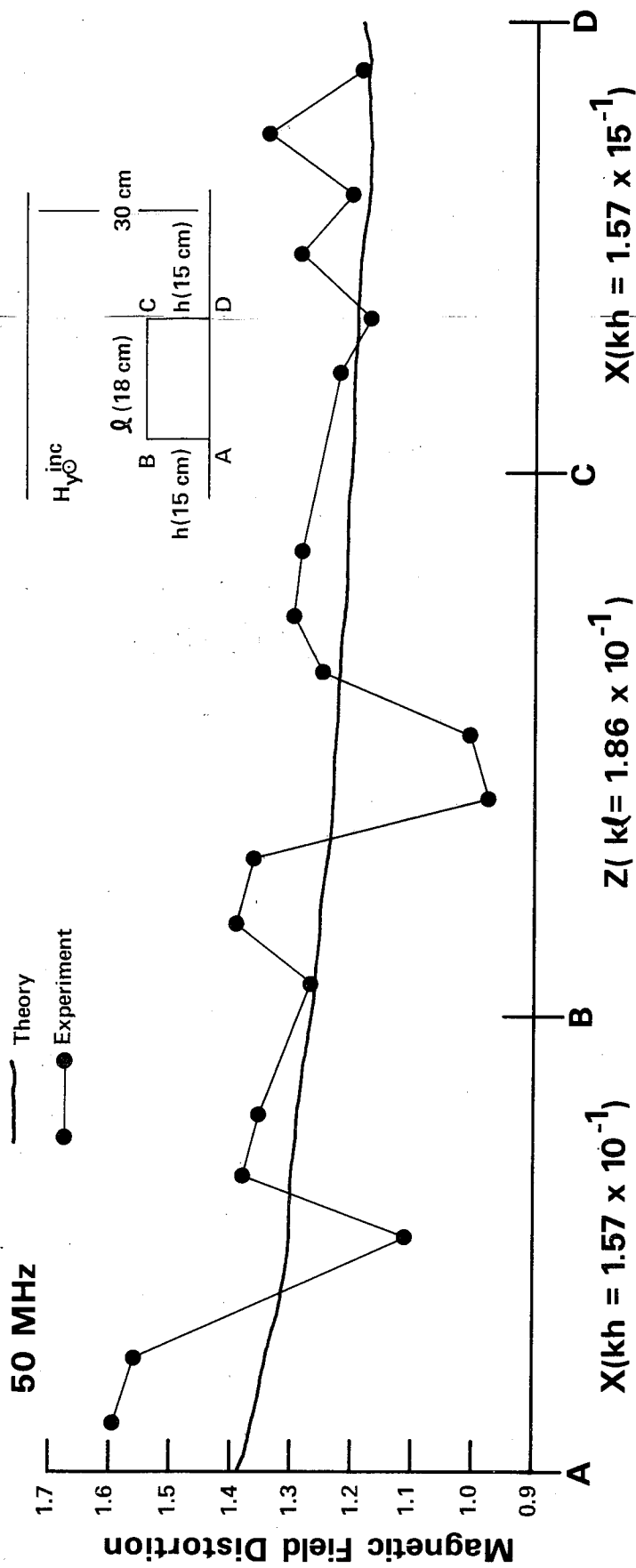


Figure 14. Magnetic field distortion due to a perfectly conducting cylinder (width $\lambda = 18\text{ cm}$, height $h = 15\text{ cm}$) in a transverse electromagnetic cell at 50 MHz.

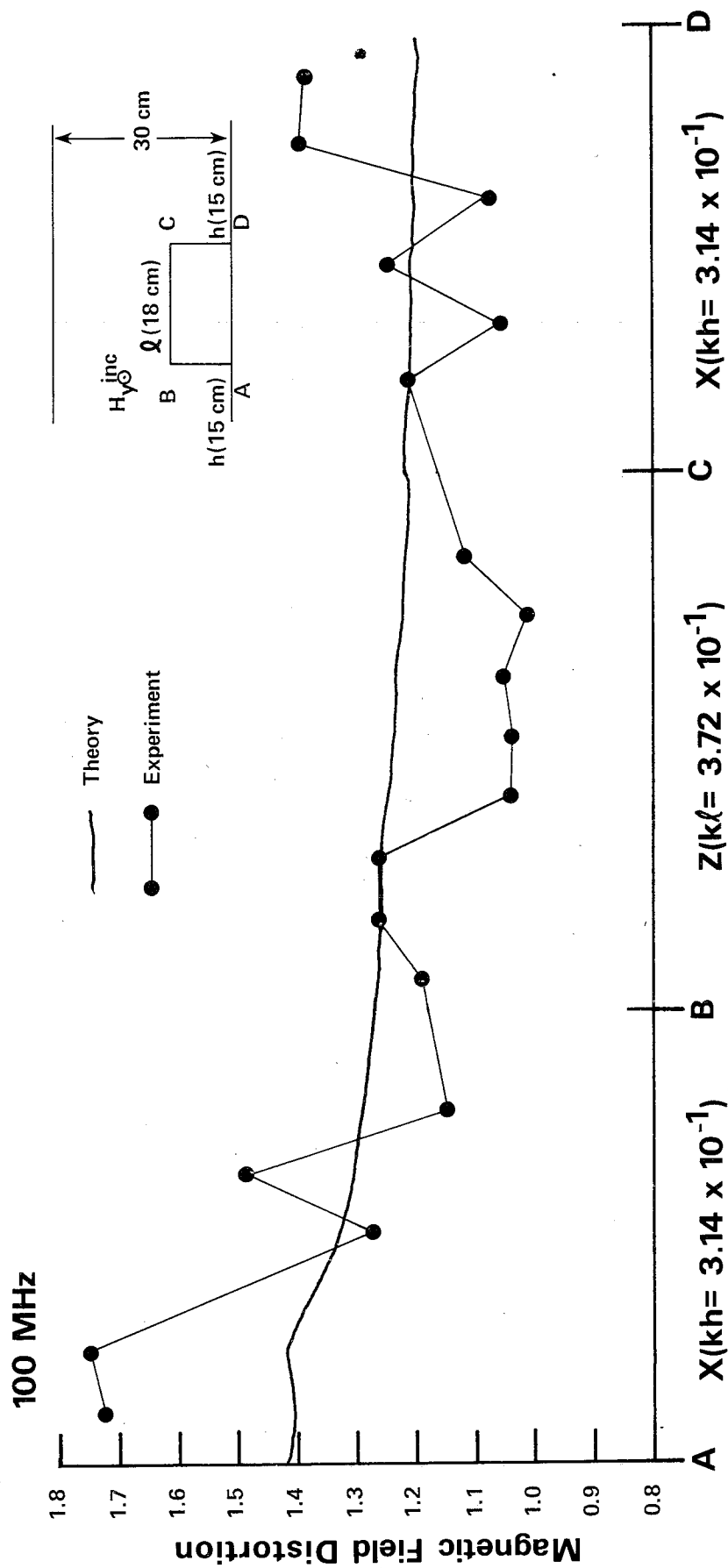


Figure 15. Magnetic field distortion due to a perfectly conducting cylinder (width $Q = 18\text{ cm}$, height $h = 15\text{ cm}$) in a transverse electromagnetic cell at 100 MHz.

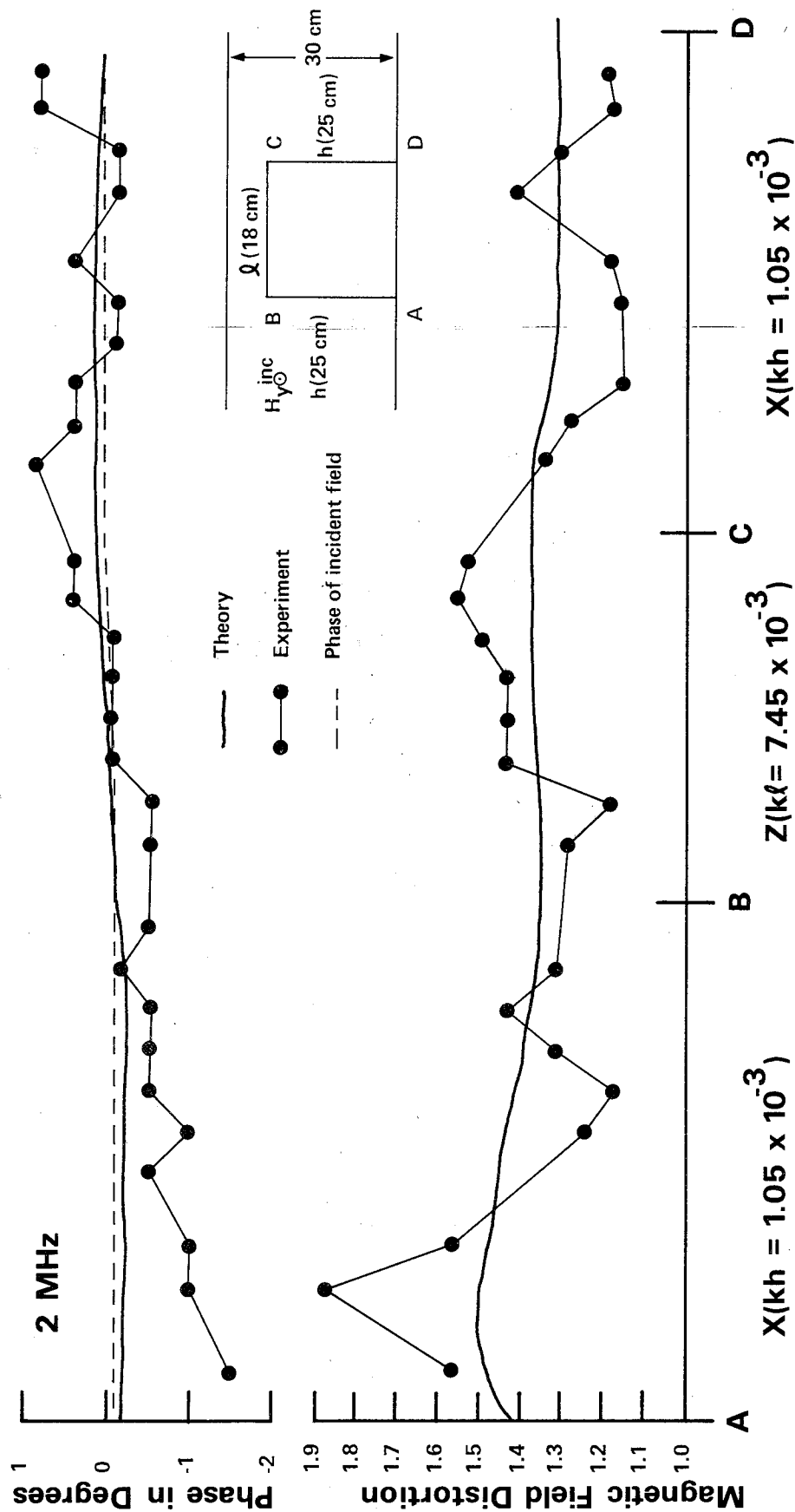


Figure 16. Magnetic field distortion due to a perfectly conducting cylinder (width $l = 18$ cm, height $h = 25$ cm) in a transverse electromagnetic cell at 2 MHz.

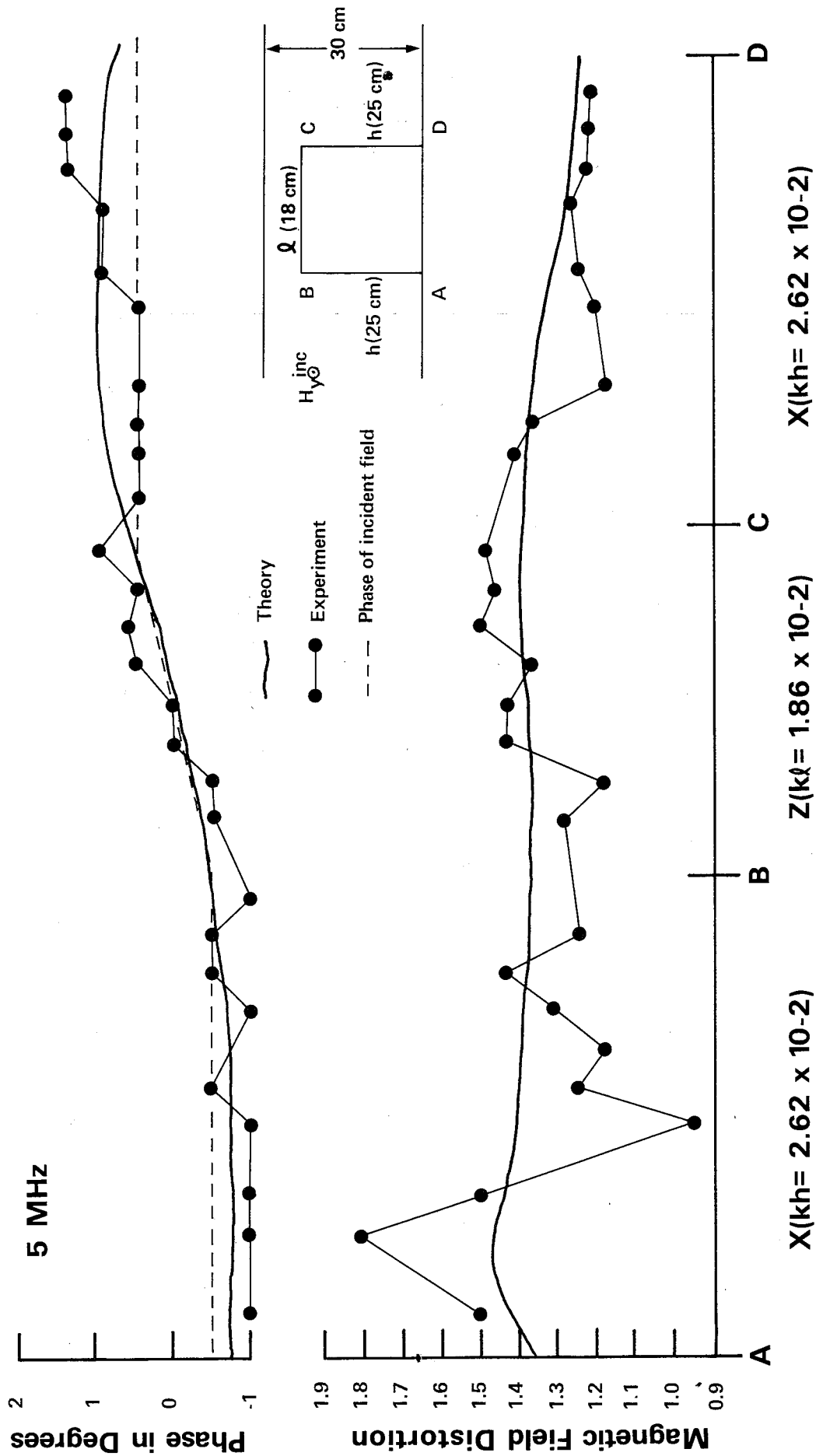


Figure 17. Magnetic field distortion due to a perfectly conducting cylinder (width $Q = 18$ cm, height $h = 25$ cm) in a transverse electromagnetic cell at 5 MHz.

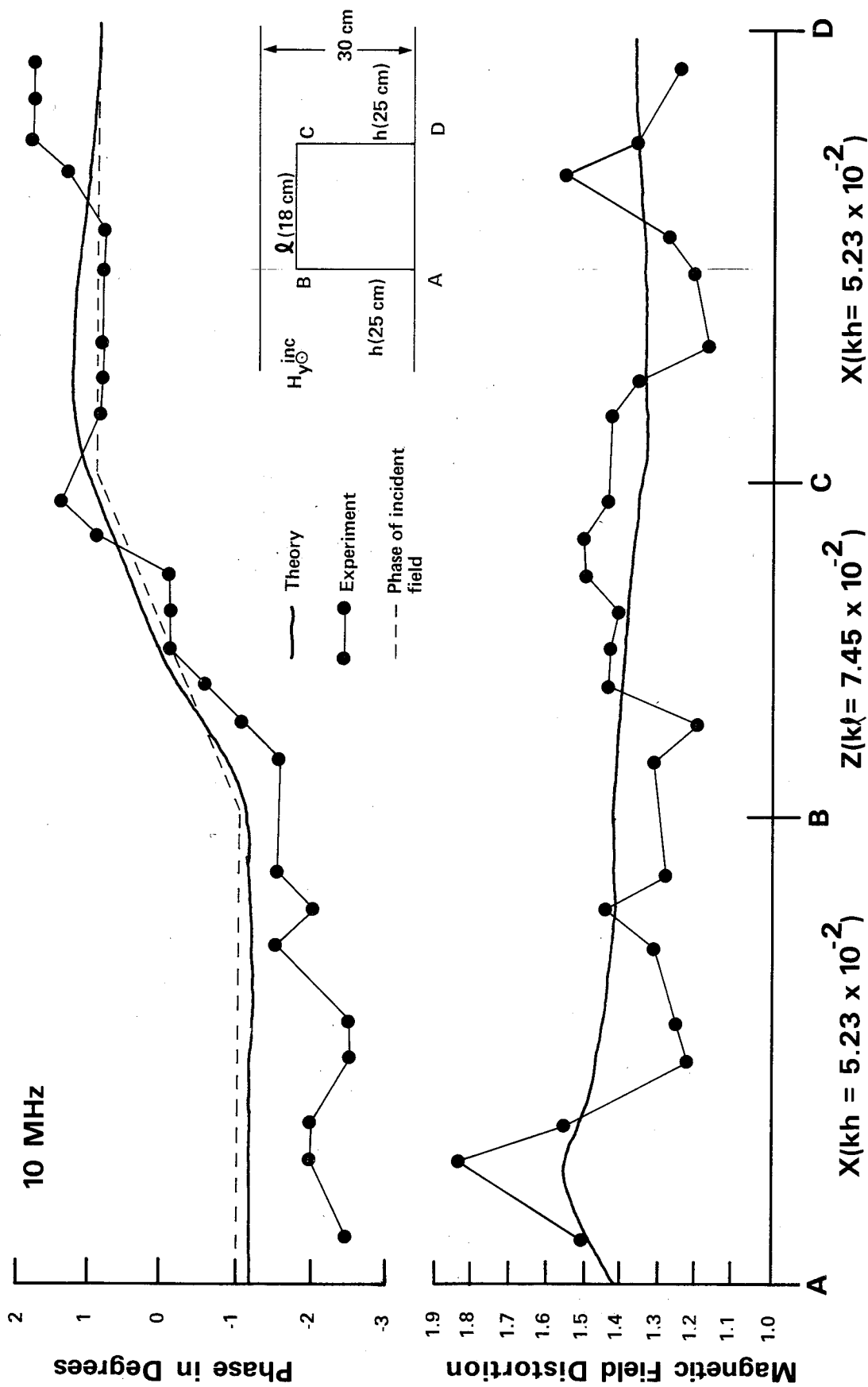


Figure 18. Magnetic field distortion due to a perfectly conducting cylinder (width $l = 18$ cm, height $h = 25$ cm) in a transverse electromagnetic cell at 10 MHz.

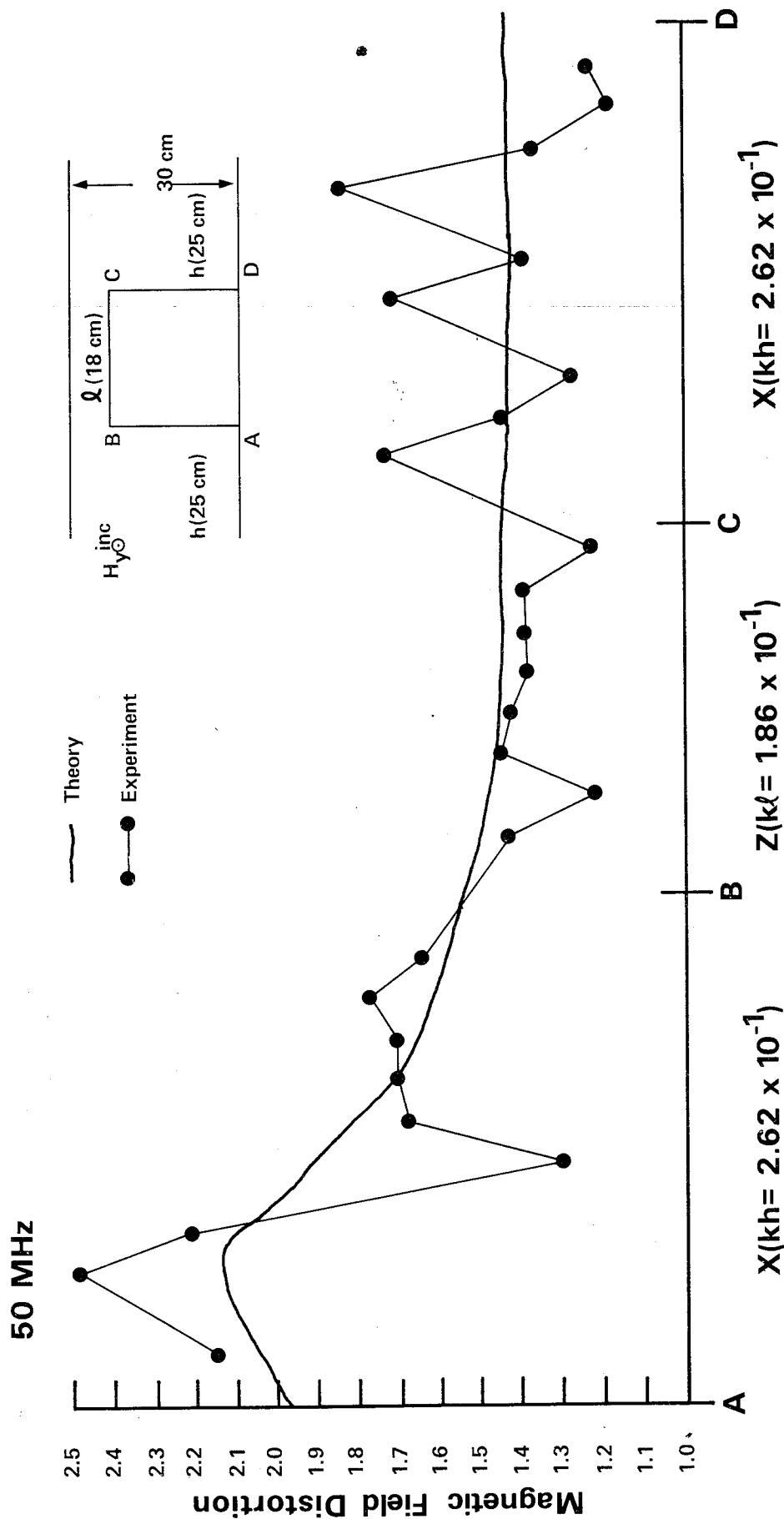


Figure 19. Magnetic field distortion due to a perfectly conducting cylinder (width $\lambda = 18$ cm, height $h = 25$ cm) in a transverse electromagnetic cell at 50 MHz.

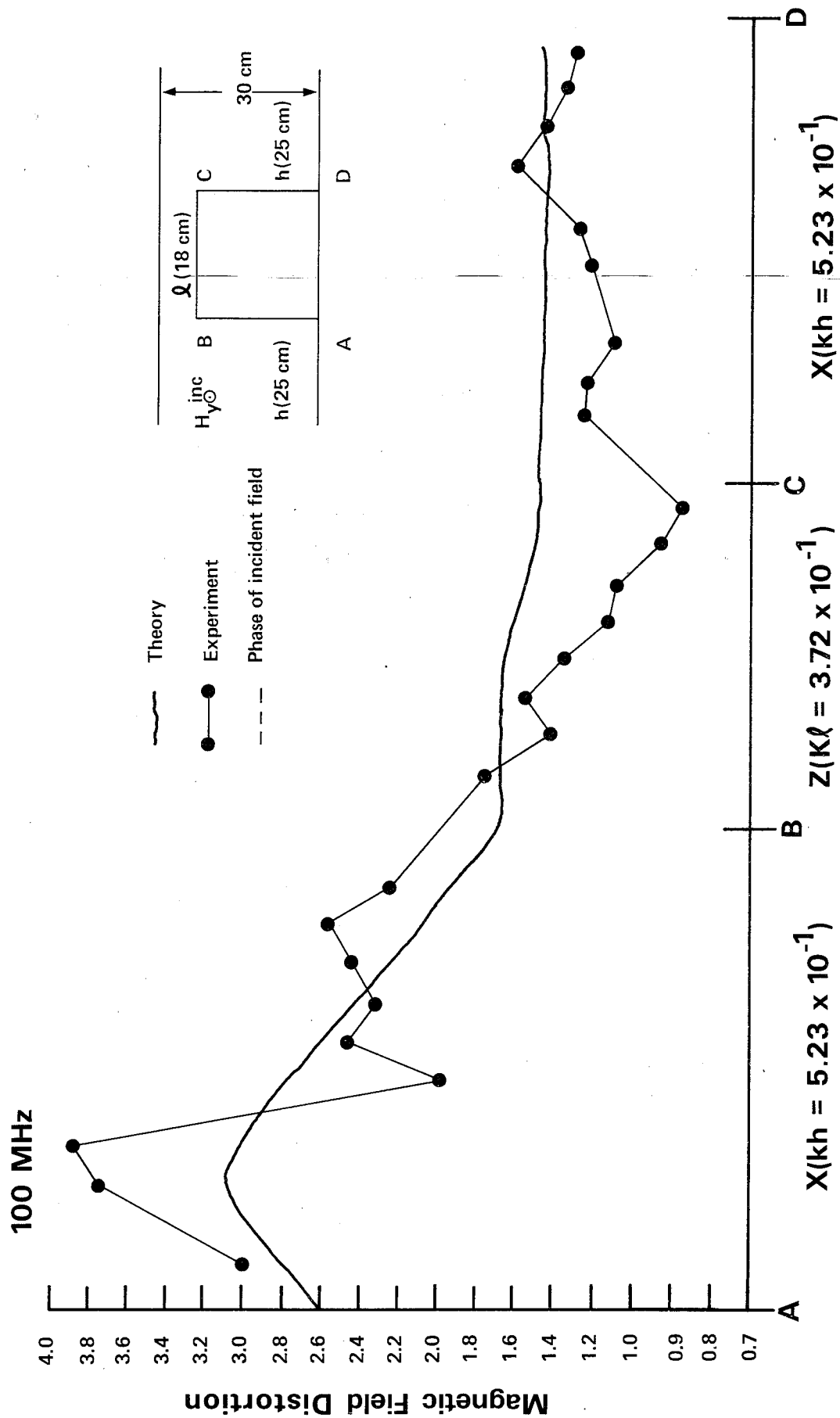


Figure 20. Magnetic field distortion due to a perfectly conducting cylinder (width $\lambda = 18$ cm, height $h = 25$ cm) in a transverse electromagnetic cell at 100 MHz.

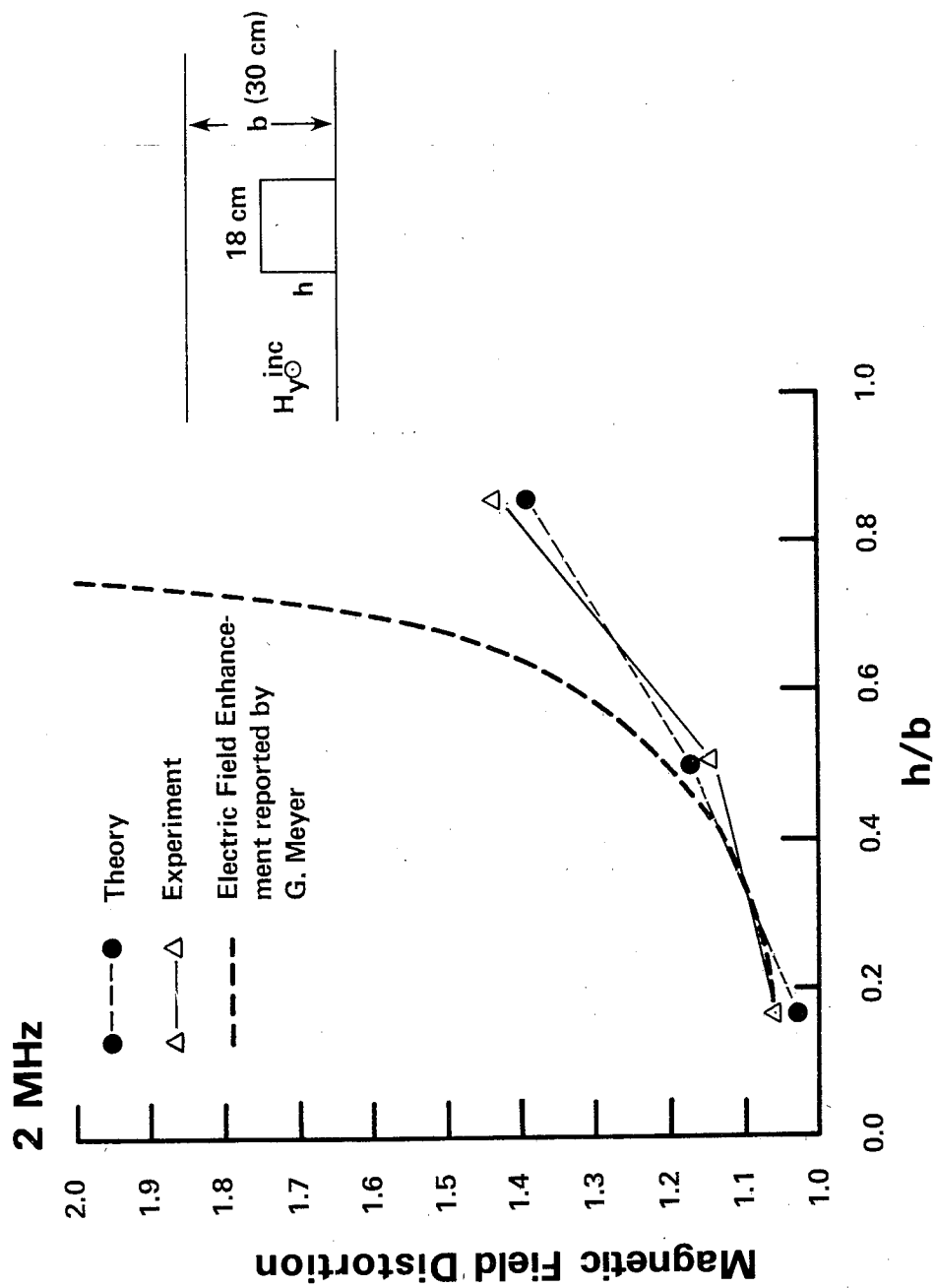


Figure 21. Magnetic field distortion at the center of the top of the cylinder as the ratio of its height to the separation distance of the parallel plate waveguide at 2 MHz.

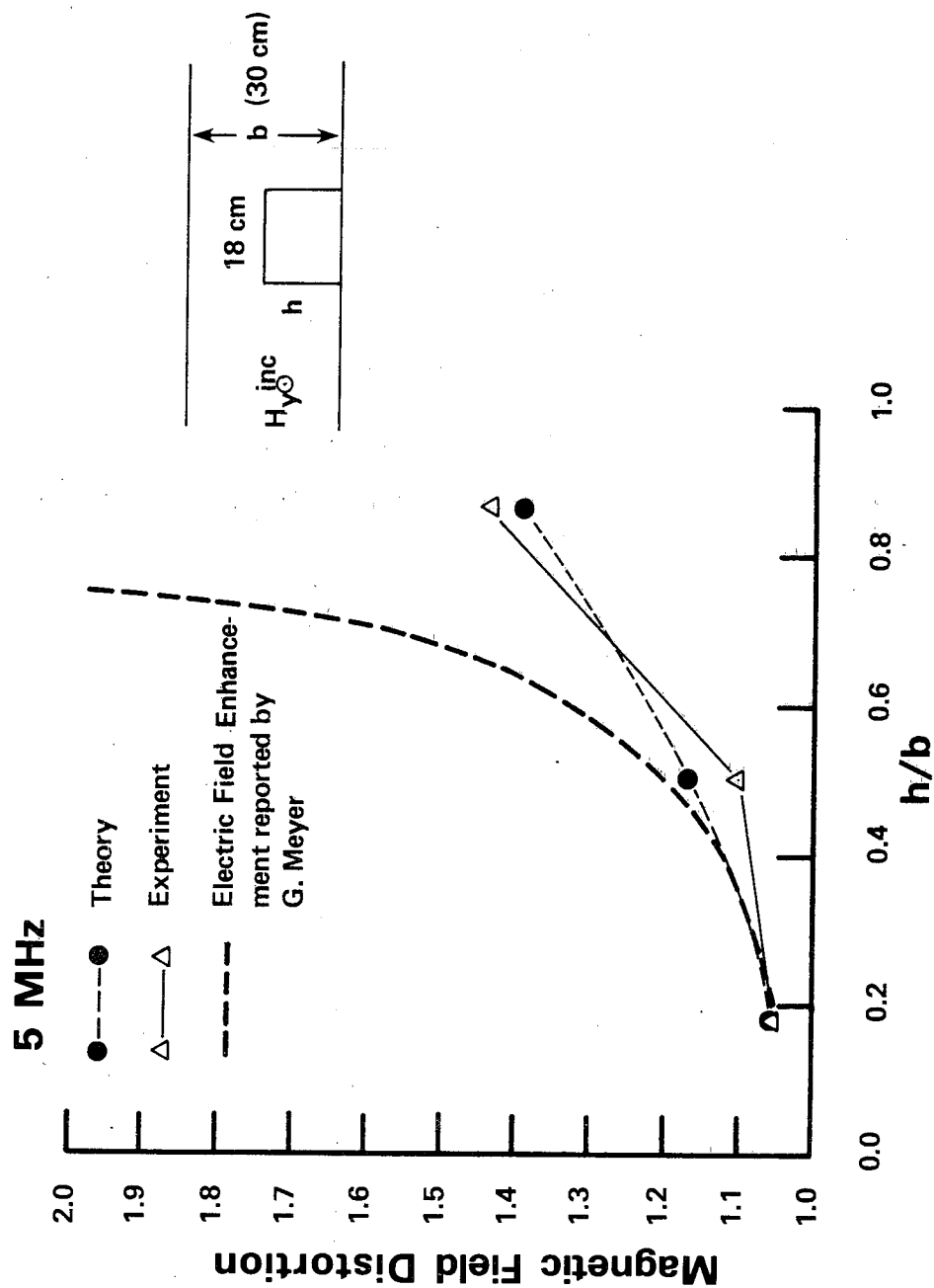


Figure 22. Magnetic field distortion at the center of the top of the cylinder as the ratio of its height to the separation distance of the parallel plate waveguide at 5 MHz.

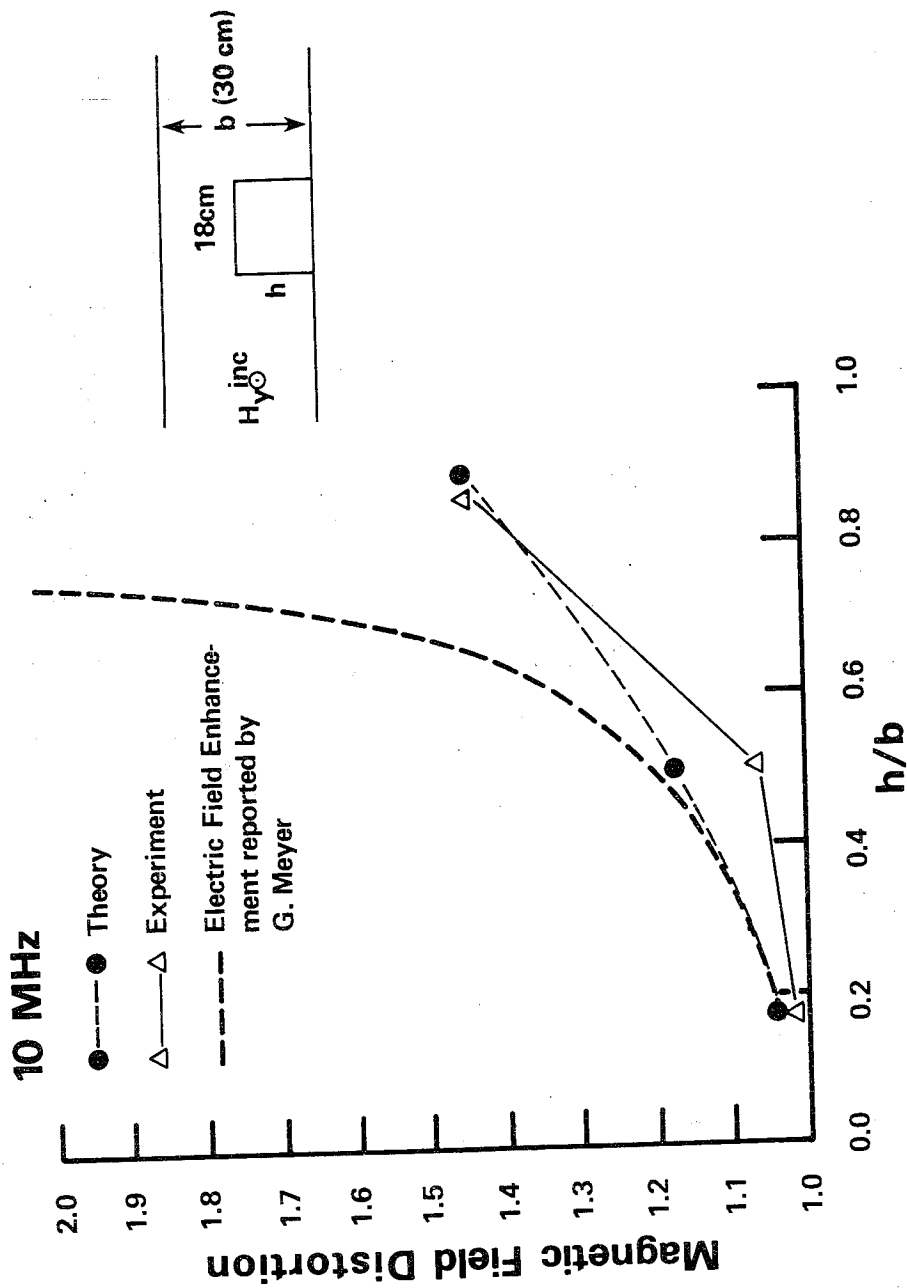


Figure 23. Magnetic field distortion at the center of the top of the cylinder as the ratio of its height to the separation distance of the parallel plate waveguide at 10 MHz.

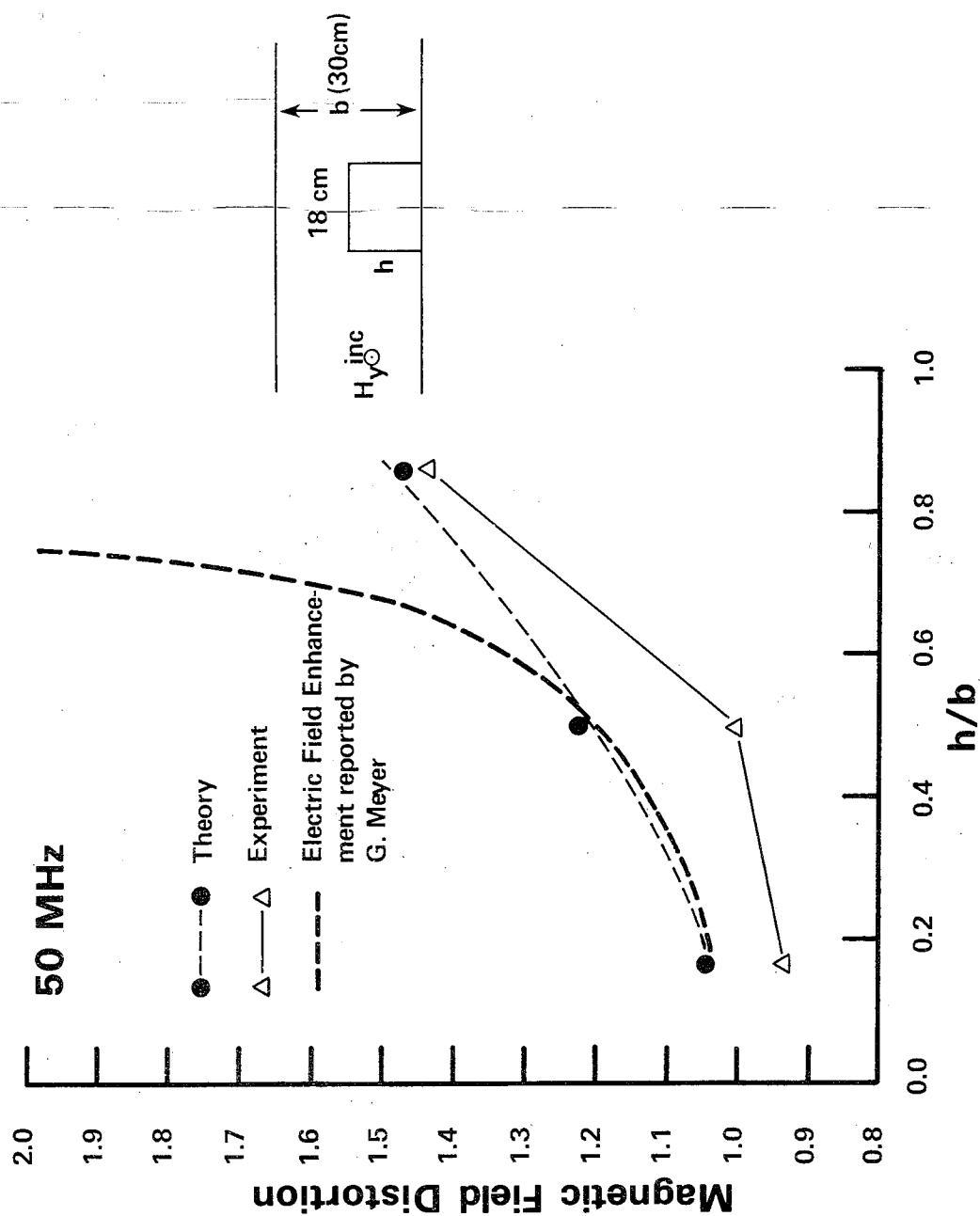


Figure 24. Magnetic field distortion at the center of the top of the cylinder as the ratio of its height to the separation distance of the parallel plate waveguide at 50 MHz.

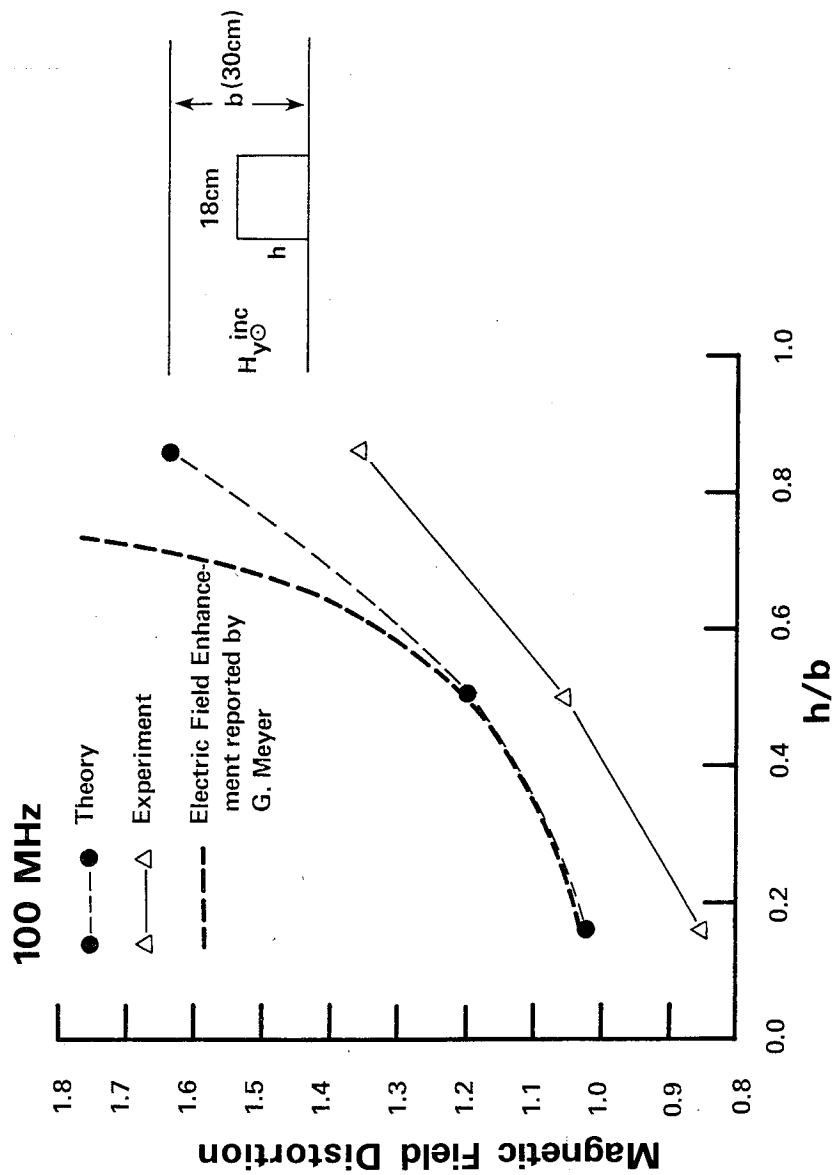


Figure 25. Magnetic field distortion at the center of the top of the cylinder as the ratio of its height to the separation distance of the parallel plate waveguide at 100 MHz.

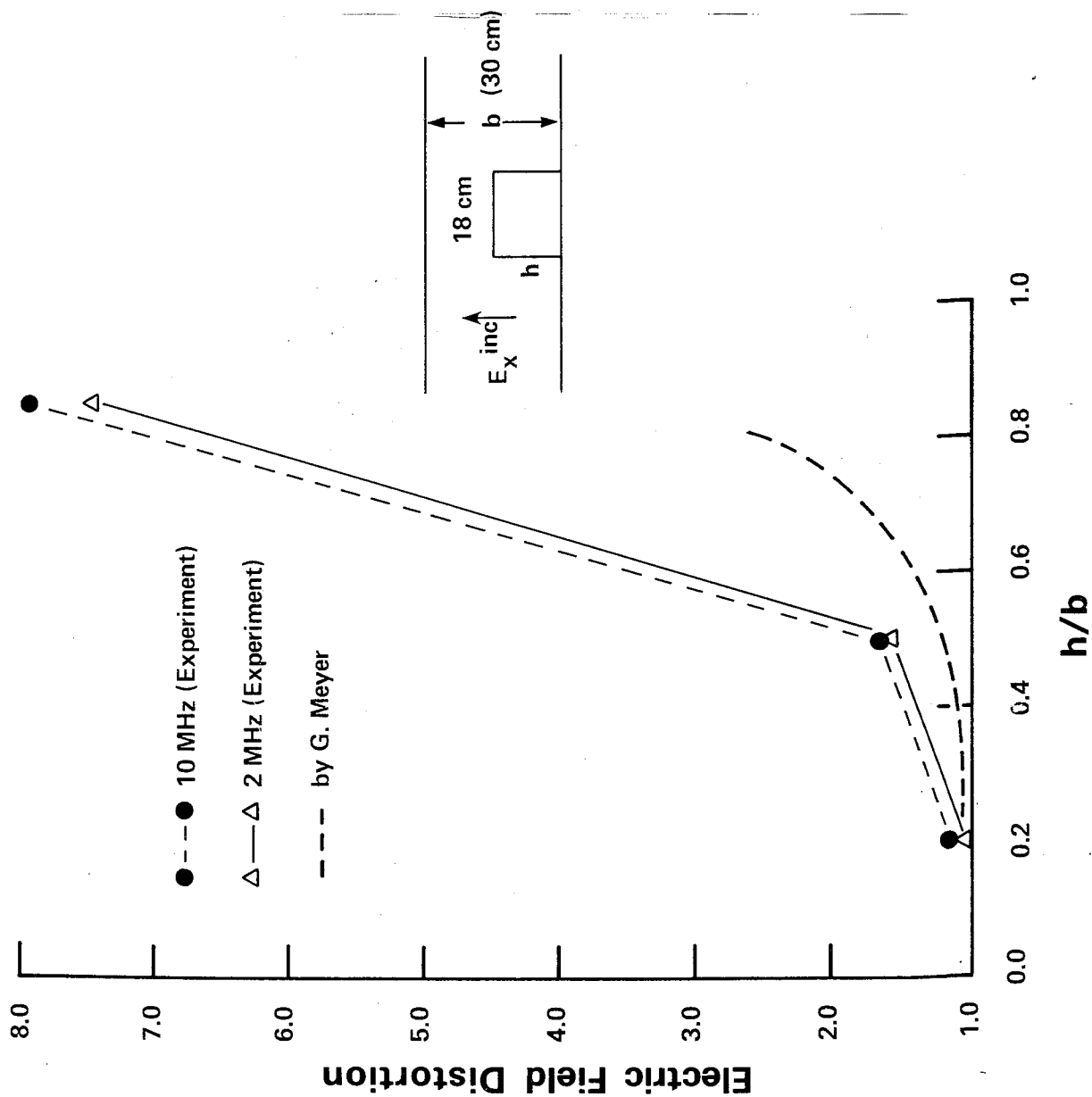


Figure 26. Electric field distortion at the center of the top of the cylinder as the ratio of its height to the separation distance of the parallel plate waveguide.

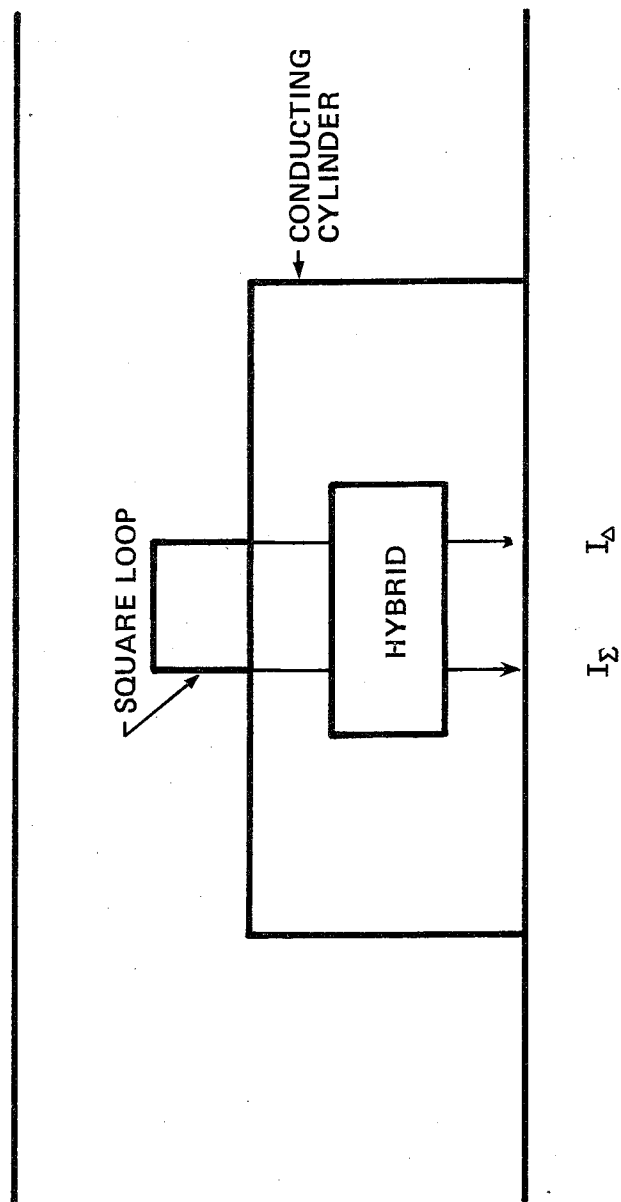


Figure 27. Simultaneous electric and magnetic field measurements using a doubly-loaded electrically small loop.

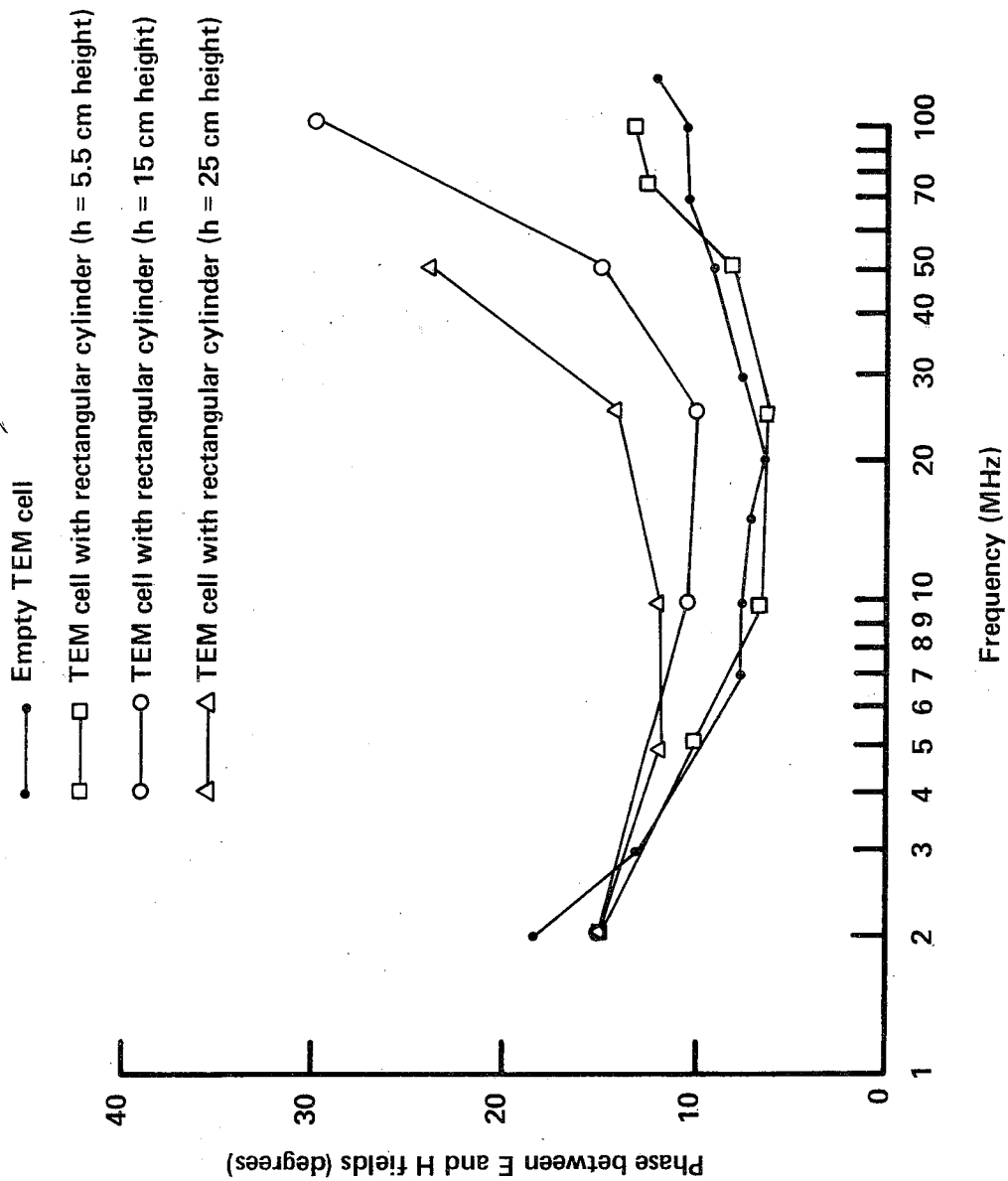


Figure 28. Phase degradation of the TEM mode as the ratio of the cylinder height to the separation distance between the center conductor and the ground plane in the TEM cell.

U.S. DEPT. OF COMM. BIBLIOGRAPHIC DATA SHEET	1. PUBLICATION OR REPORT NO. NBS TN-1028	2. Gov't. Accession No.	3. Recipient's Accession No.
4. TITLE AND SUBTITLE Theoretical and Experimental Investigations of Electro- magnetic Field Distortion Due to a Perfectly Conducting Rectangular Cylinder in a Transverse Electromagnetic Cell.		5. Publication Date April 1981	
7. AUTHOR(S) Motohisa Kanda		6. Performing Organization Code	
9. PERFORMING ORGANIZATION NAME AND ADDRESS NATIONAL BUREAU OF STANDARDS DEPARTMENT OF COMMERCE WASHINGTON, DC 20234		8. Performing Organ. Report No.	
12. SPONSORING ORGANIZATION NAME AND COMPLETE ADDRESS (Street, City, State, ZIP)		10. Project/Task/Work Unit No. 7233182	
15. SUPPLEMENTARY NOTES <input type="checkbox"/> Document describes a computer program; SF-185, FIPS Software Summary, is attached.		11. Contract/Grant No.	
16. ABSTRACT (A 200-word or less factual summary of most significant information. If document includes a significant bibliography or literature survey, mention it here.) The study of electromagnetic compatibility (EMC), that is the electronic and biological effects due to electromagnetic (EM) radiation, and EM calibration require accurate EM measurement techniques for defining the EM interference (EM) characteristics. Thus, fully enclosed rectangular transverse electromagnetic (TEM) transmission lines with thin inner conductors are often used for generating standard known test fields. In all cases it is desirable that only the dominant TEM mode should propagate. In the EMC measurements, an object under test is placed inside of a TEM cell. The field from the TEM mode incident upon this scattering object is identical to that of a plane wave in a free space. However, the scattered field produced by the object in the TEM cell is different from the scattered field produced by the object in a free space, because of multiple reflections from the TEM cell walls, or equivalently, the mutual coupling between the object and the TEM cell. The purpose of this paper is to discuss the loading effects, i.e., the electromagnetic field distortion caused by an object under test in a TEM cell. In the theoretical analysis, the frequency domain integral equation for the magnetic field, or equivalently, the current density on the surface of a perfectly conducting cylinder in a parallel plate waveguide is solved by the method of moments to predict the degree of magnetic field distortion. The experimental investigations are performed by mounting a number of electrically small half loops on the surface of the perfectly conducting cylinder in a TEM cell. The loading effects in terms of magnetic field distortion are analyzed as the ratio of one of the object dimensions (height) to the separation distance between the inner conductor and the ground plane of the TEM cell. Also, the response of an electrically small loop to both the magnetic and electric components of the electromagnetic field is used to measure the phase relation between the magnetic and electric fields, which in turn can be used to determine the degree of degradation of the TEM mode due to the presence of the perfectly conducting cylinder. These theoretical and experimental results are compared with the available quasi electrostatic results.		13. Type of Report & Period Covered	
		14. Sponsoring Agency Code	
17. KEY WORDS (six to twelve entries; alphabetical order; capitalize only the first letter of the first key word unless a proper name; separated by semicolons) Electromagnetic Compatibility (EMC); Green's function; integral equation; linear equation; method of moments; parallel plate waveguide; quasi electrostatic; TEM cell.			
18. AVAILABILITY <input checked="" type="checkbox"/> Unlimited <input type="checkbox"/> For Official Distribution. Do Not Release to NTIS <input checked="" type="checkbox"/> Order From Sup. of Doc., U.S. Government Printing Office, Washington, DC 20402 <input type="checkbox"/> Order From National Technical Information Service (NTIS), Springfield, VA. 22161		19. SECURITY CLASS (THIS REPORT) UNCLASSIFIED 20. SECURITY CLASS (THIS PAGE) UNCLASSIFIED	21. NO. OF PRINTED PAGES 48 22. Price \$2.50

USCOMM-DC

